Supporting information: Histogram-free reweighting with grand canonical Monte Carlo: Post-simulation optimization of non-bonded potentials for phase equilibria

Richard A. Messerly,[*,†] Mohammad S. Barhaghi,[‡] Jeffrey J. Potoff,[‡] and Michael R. Shirts[¶]

†*Thermodynamics Research Center, National Institute of Standards and Technology, Boulder, Colorado, 80305, United States*

‡*Department of Chemical Engineering and Materials Science, Wayne State University, Detroit, Michigan 48202, United States*

¶*Department of Chemical and Biological Engineering, University of Colorado, Boulder, Colorado, 80309, United States*

E-mail: richard.messerly@nist.gov

SI.I Bonded parameters

Table SI.I: Equilibrium (fixed) bond lengths (r_{eq}). CH_x and CH_y represent CH_3, $CH_2(sp^3)$, $CH(sp^3)$, or $C(sp^3)$ sites.

Bond sites	r_{eq} (nm)		
	TraPPE	MiPPE	NERD
CH_x-CH_y	0.154	0.154	0.154
C(sp)-CH_x	–	0.146	–
CH≡CH	–	0.121	–
C≡CH	–	0.121	–

Table SI.II: Equilibrium bond angles (θ_{eq}) and force constants $(k_\theta/k_{\mathrm{B}})$, where k_{B} is the Boltzmann constant.

Bending sites	θ_{eq} (degrees)			k_θ/k_{B} (K/rad^2)
	TraPPE	MiPPE	NERD	
CH_x-CH_2-CH_y	114.0	114.0	114.0	62500
CH_x-CH-CH_y	112.0	112.0	109.5	62500
CH_x-C-CH_y	109.5	109.5	109.5	62500
CH_x-CH_2-C(sp)	–	112	–	62500
CH_x-C(sp)≡CH	–	180	–	30800
CH_x-C(sp)≡C	–	180	–	30800

Table SI.III: Fourier constants (c_n/k_{B}) in units of K.

Torsion sites	c_0/k_{B}	c_1/k_{B}	c_2/k_{B}	c_3/k_{B}
CH_x-CH_2-CH_2-CH_y	0.0	355.03	-68.19	791.32
CH_x-CH_2-CH-CH_y	-251.06	428.73	-111.85	441.27
CH_x-CH_2-C-CH_y	0.0	0.0	0.0	461.29
CH_x-CH-CH-CH_y	-251.06	428.73	-111.85	441.27
CH_x-CH_2-CH_2-C(sp)	94.88	162.00	-205.40	980.40
CH_x-CH_2-C(sp)≡C(sp)	0	0	0	0
CH_x-CH_2-C(sp)≡CH(sp)	0	0	0	0
CH_x-C(sp)≡C(sp)-CH_y	0	0	0	0

SI.II Compiler and hardware

With the exception of the 20 replicates performed for MiPPE cyclohexane, all simulations are run on a Linux 4.4.0-112-generic x86_64 on an Intel(R) Xeon(R) CPU E5-2699 v4 @ 2.20GHz machine. On this machine, GOMC was erroneously compiled using the sub-optimal GNU compiler collection (GCC) instead of the preferred Intel compiler. GOMC compiled with the Intel compiler typically runs approximately twice as fast as GOMC compiled with the GCC compiler.

The 20 replicate simulations for MiPPE cyclohexane utilize several different machine hardware architectures, listed in Table SI.IV. GOMC was compiled with the Intel compiler on each of these machines.

Table SI.IV: Machine hardware for 20 replicate simulations of MiPPE cyclohexane

Intel(R) Core(TM) i7-4790K CPU @ 4.00GHz
Intel(R) Core(TM) i5-3570 CPU @ 3.40GHz
Intel(R) Core(TM) i5-2500K CPU @ 3.30GHz
Intel(R) Xeon(R) CPU X5450 @ 3.00GHz
Intel(R) Xeon(R) CPU X5355 @ 2.66GHz
Intel(R) Xeon(R) CPU E5-2640 v3 @ 2.60GHz
Intel(R) Core(TM)2 Quad CPU Q6600 @ 2.40GHz

SI.III ϵ-scaling

SI.III.1 Tabulated ψ values

Table SI.V: Optimal ϵ-scaling parameter (ψ) values and corresponding scoring function. Abbreviations correspond to those in Figure 2.

Molecular name	Abbreviation	Optimal ψ	Optimal score
Branched alkanes			
2-methylpropane	$2MC_3$	1.0015	0.3883
2-methylbutane	$2MC_4$	1.0025	0.4281
2-methylpentane	$2MC_5$	1.0020	0.4770
3-methylpentane	$3MC_5$	1.0103	0.4050
2,2-dimethylpropane	$22DMC_3$	1.0035	0.5132
2,2-dimethylbutane	$22DMC_4$	0.9985	0.5445
2,3-dimethylbutane	$23DMC_4$	1.0000	0.4724
2,2,4-trimethylpentane	$234TMC_5$	1.0005	0.4367
Alkynes			
1-ethyne	C_2	1.0005	0.2931
1-propyne	C_3	0.9965	0.3307
1-butyne	$1C_4$	1.0063	1.143
2-butyne	$2C_4$	1.0031	0.3191
1-pentyne	$1C_5$	1.0087	1.8505
2-pentyne	$2C_5$	1.0186	1.3801
1-hexyne	$1C_6$	1.0063	1.908
2-hexyne	$2C_6$	1.0228	1.0594
1-heptyne	$1C_7$	1.0066	0.8415
1-octyne	$1C_8$	1.0034	0.9777
1-nonyne	$1C_9$	1.0000	0.9128

SI.III.2 Tabulated phase equilibria for optimal ψ

SI.IV Case study: Cyclohexane optimization

SI.IV.1 Minimum number of effective snapshots

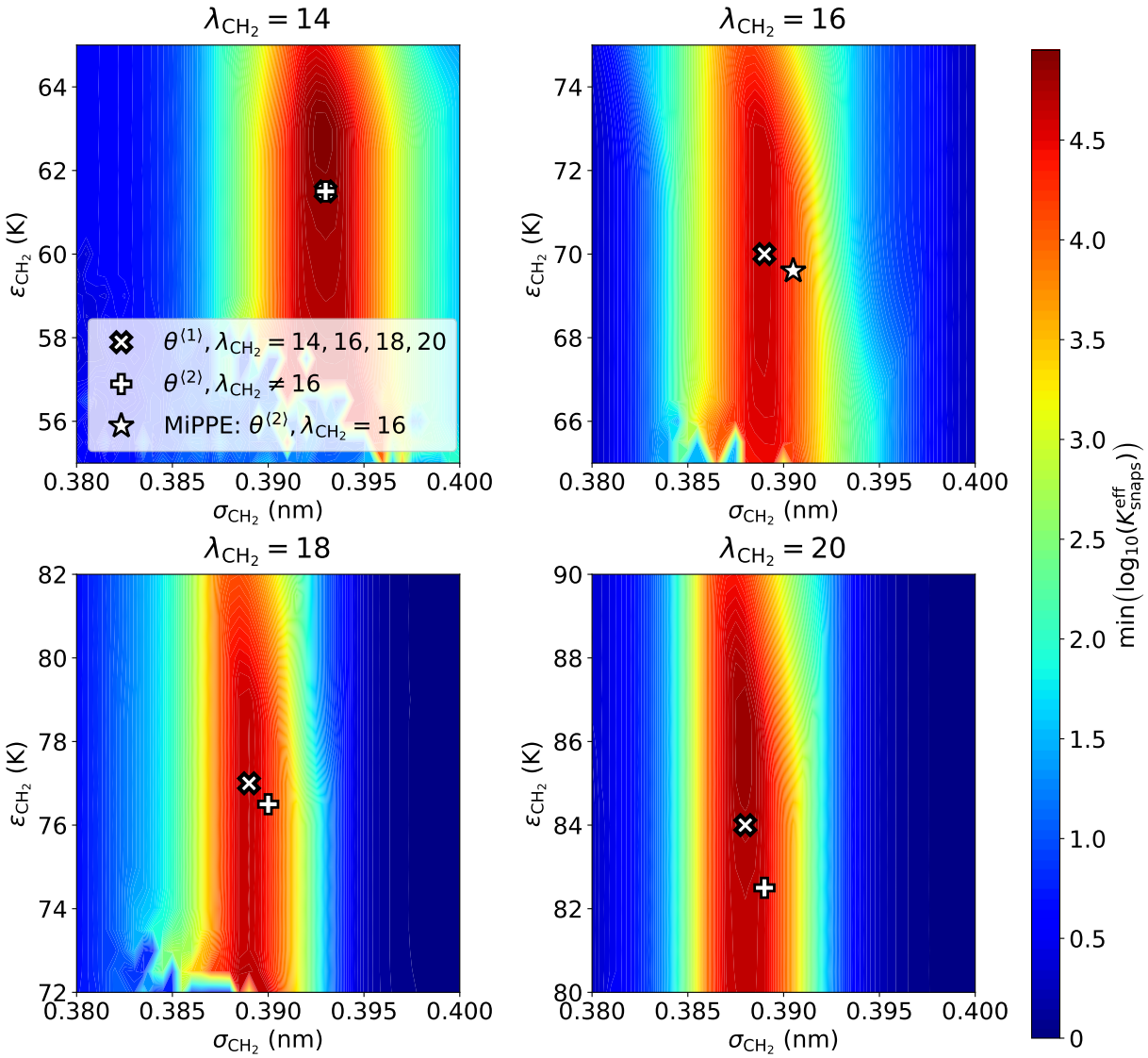

Figure SI.1: Second iteration minimum number of effective snapshots $(\min(K^{\text{eff}}_{\text{snaps}}))$ with respect to ϵ_{CH_2} and σ_{CH_2} for cyclohexane. Optimization has converged as $\min(K^{\text{eff}}_{\text{snaps}}) \gg 50$ for the optimal ϵ_{CH_2}, σ_{CH_2}, λ_{CH_2} parameter set. Top-left, top-right, bottom-left, and bottom-right panels correspond $\lambda_{CH_2} = 14$, $\lambda_{CH_2} = 16$, $\lambda_{CH_2} = 18$, and $\lambda_{CH_2} = 12$, respectively. White star represents the optimal parameter set, i.e., the lowest value of S, for a given λ_{CH_2}

SI.IV.2 Tabulated phase equilibria for iterations

Table SI.VI: GCMC-MBAR results for the MiPPE force field (second iteration, $\theta^{\langle 2 \rangle}$ $\lambda_{\mathrm{CH_2}} = 16$). Subscripts correspond to the 95% confidence interval computed with twenty independent replicate GCMC simulations at each state point.

T^{sat} (K)	$\rho_{\mathrm{liq}}^{\mathrm{sat}}$ (kg/m^3)	$\rho_{\mathrm{vap}}^{\mathrm{sat}}$ (kg/m^3)	$P_{\mathrm{vap}}^{\mathrm{sat}}$ (MPa)	ΔH_{v} (kJ/mol)	$Z_{\mathrm{vap}}^{\mathrm{sat}}$

Table SI.VII: GCMC-MBAR results for the TraPPE force field (zeroth iteration, $\theta^{\langle 0 \rangle}$). Subscripts correspond to the 95% confidence interval computed with bootstrap re-sampling.

T^{sat} (K)	$\rho_{\mathrm{liq}}^{\mathrm{sat}}$ (kg/m^3)	$\rho_{\mathrm{vap}}^{\mathrm{sat}}$ (kg/m^3)	$P_{\mathrm{vap}}^{\mathrm{sat}}$ (MPa)	ΔH_{v} (kJ/mol)	$Z_{\mathrm{vap}}^{\mathrm{sat}}$
360	$709.02_{0.33}$	$4.775_{0.062}$	$1.606_{0.016}$	$26.916_{0.050}$	$0.946_{0.016}$
370	$698.93_{0.39}$	$6.067_{0.072}$	$2.079_{0.012}$	$26.440_{0.042}$	$0.937_{0.012}$
380	$688.03_{0.44}$	$7.610_{0.088}$	$2.65_{0.01}$	$25.919_{0.036}$	$0.927_{0.011}$
390	$677.14_{0.49}$	$9.43_{0.11}$	$3.33_{0.01}$	$25.382_{0.033}$	$0.916_{0.010}$
400	$666.43_{0.55}$	$11.57_{0.12}$	$4.13_{0.01}$	$24.835_{0.030}$	$0.90_{0.01}$
410	$655.56_{0.39}$	$14.07_{0.13}$	$5.071_{0.017}$	$24.266_{0.023}$	$0.89_{0.01}$
420	$644.33_{0.48}$	$16.97_{0.13}$	$6.158_{0.025}$	$23.665_{0.027}$	$0.87_{0.01}$
430	$632.76_{0.54}$	$20.32_{0.12}$	$7.408_{0.031}$	$23.030_{0.030}$	$0.86_{0.01}$
440	$620.79_{0.67}$	$24.18_{0.26}$	$8.833_{0.039}$	$22.356_{0.051}$	$0.84_{0.01}$
450	$608.2_{1.2}$	$28.64_{0.96}$	$10.450_{0.052}$	$21.63_{0.10}$	$0.821_{0.028}$
460	$595.0_{2.9}$	$33.8_{2.4}$	$12.271_{0.098}$	$20.85_{0.20}$	$0.799_{0.057}$
470	$581.0_{4.6}$	$39.7_{3.8}$	$14.31_{0.17}$	$20.01_{0.30}$	$0.776_{0.075}$
480	$566.2_{4.8}$	$46.7_{4.6}$	$16.59_{0.24}$	$19.08_{0.33}$	$0.750_{0.074}$
490	$550.4_{4.5}$	$54.8_{4.7}$	$19.12_{0.29}$	$18.06_{0.38}$	$0.720_{0.063}$
500	$533.2_{5.4}$	$64.6_{3.8}$	$21.93_{0.38}$	$16.913_{0.088}$	$0.687_{0.042}$
510	$513.8_{5.3}$	$76.6_{5.4}$	$25.04_{0.37}$	$15.59_{0.33}$	$0.649_{0.047}$
520	$491.6_{3.8}$	$91.4_{7.6}$	$28.48_{0.28}$	$14.08_{0.34}$	$0.607_{0.051}$

Table SI.VIII: GCMC-MBAR results for the first iteration ($\theta^{\langle 1 \rangle}$) $\lambda_{\mathrm{CH_2}} = 14$ force field. Subscripts correspond to the 95% confidence interval computed with bootstrap re-sampling.

T^{sat} (K)	$\rho_{\mathrm{liq}}^{\mathrm{sat}}$ (kg/m^3)	$\rho_{\mathrm{vap}}^{\mathrm{sat}}$ (kg/m^3)	$P_{\mathrm{vap}}^{\mathrm{sat}}$ (MPa)	ΔH_{v} (kJ/mol)	$Z_{\mathrm{vap}}^{\mathrm{sat}}$
360	$704.93_{0.26}$	$3.743_{0.073}$	$1.271_{0.044}$	$28.78_{0.10}$	$0.955_{0.038}$
370	$695.36_{0.63}$	$4.822_{0.057}$	$1.669_{0.048}$	$28.28_{0.11}$	$0.947_{0.029}$
380	$684.68_{0.79}$	$6.125_{0.057}$	$2.157_{0.049}$	$27.73_{0.11}$	$0.938_{0.023}$
390	$673.71_{0.68}$	$7.680_{0.084}$	$2.745_{0.048}$	$27.144_{0.099}$	$0.928_{0.019}$
400	$663.17_{0.45}$	$9.52_{0.13}$	$3.445_{0.044}$	$26.568_{0.086}$	$0.916_{0.017}$
410	$652.73_{0.24}$	$11.68_{0.17}$	$4.273_{0.039}$	$25.980_{0.062}$	$0.903_{0.016}$
420	$641.98_{0.82}$	$14.21_{0.23}$	$5.240_{0.033}$	$25.360_{0.039}$	$0.889_{0.015}$
430	$630.8_{1.2}$	$17.15_{0.30}$	$6.362_{0.032}$	$24.703_{0.036}$	$0.873_{0.016}$
440	$619.3_{1.1}$	$20.57_{0.39}$	$7.652_{0.041}$	$24.005_{0.044}$	$0.856_{0.017}$
450	$607.24_{0.80}$	$24.53_{0.54}$	$9.125_{0.062}$	$23.261_{0.063}$	$0.837_{0.019}$
460	$594.62_{0.73}$	$29.11_{0.77}$	$10.796_{0.093}$	$22.463_{0.085}$	$0.816_{0.023}$
470	$581.33_{0.87}$	$34.4_{1.1}$	$12.68_{0.14}$	$21.60_{0.11}$	$0.793_{0.027}$
480	$567.3_{1.1}$	$40.6_{1.6}$	$14.80_{0.21}$	$20.68_{0.13}$	$0.768_{0.032}$
490	$552.4_{1.5}$	$47.9_{2.1}$	$17.16_{0.30}$	$19.66_{0.14}$	$0.741_{0.035}$
500	$536.3_{2.5}$	$56.5_{2.6}$	$19.80_{0.41}$	$18.52_{0.14}$	$0.709_{0.036}$
510	$518.2_{4.3}$	$67.2_{2.8}$	$22.73_{0.54}$	$17.20_{0.16}$	$0.672_{0.033}$

Table SI.IX: GCMC-MBAR results for the first iteration ($\theta^{\langle 1 \rangle}$) $\lambda_{\mathrm{CH_2}} = 16$ force field. Subscripts correspond to the 95% confidence interval computed with bootstrap re-sampling.

T^{sat} (K)	$\rho_{\mathrm{liq}}^{\mathrm{sat}}$ (kg/m^3)	$\rho_{\mathrm{vap}}^{\mathrm{sat}}$ (kg/m^3)	$P_{\mathrm{vap}}^{\mathrm{sat}}$ (MPa)	ΔH_{v} (kJ/mol)	$Z_{\mathrm{vap}}^{\mathrm{sat}}$
360	$713.64_{0.38}$	$3.583_{0.049}$	$1.225_{0.039}$	$29.59_{0.13}$	$0.961_{0.033}$
370	$704.1_{1.2}$	$4.647_{0.057}$	$1.617_{0.036}$	$29.065_{0.088}$	$0.952_{0.024}$
380	$695.0_{2.4}$	$5.943_{0.071}$	$2.102_{0.032}$	$28.551_{0.098}$	$0.942_{0.018}$
390	$685.2_{2.3}$	$7.505_{0.090}$	$2.692_{0.027}$	$27.993_{0.084}$	$0.931_{0.015}$
400	$674.3_{1.1}$	$9.37_{0.11}$	$3.400_{0.024}$	$27.376_{0.037}$	$0.918_{0.013}$
410	$662.91_{0.76}$	$11.57_{0.12}$	$4.241_{0.026}$	$26.717_{0.040}$	$0.905_{0.011}$
420	$651.2_{1.0}$	$14.16_{0.14}$	$5.229_{0.032}$	$26.027_{0.065}$	$0.890_{0.011}$
430	$639.4_{1.1}$	$17.19_{0.18}$	$6.378_{0.040}$	$25.310_{0.078}$	$0.873_{0.011}$
440	$627.31_{0.89}$	$20.71_{0.22}$	$7.704_{0.050}$	$24.565_{0.072}$	$0.856_{0.011}$
450	$614.82_{0.58}$	$24.79_{0.24}$	$9.223_{0.059}$	$23.777_{0.051}$	$0.84_{0.01}$
460	$601.71_{0.56}$	$29.53_{0.25}$	$10.952_{0.067}$	$22.935_{0.053}$	$0.82_{0.01}$
470	$587.98_{0.65}$	$35.03_{0.48}$	$12.907_{0.067}$	$22.033_{0.094}$	$0.794_{0.012}$
480	$573.59_{0.74}$	$41.45_{0.99}$	$15.106_{0.063}$	$21.06_{0.15}$	$0.768_{0.019}$
490	$558.19_{0.80}$	$49.0_{1.7}$	$17.571_{0.086}$	$19.99_{0.20}$	$0.740_{0.026}$
500	$541.27_{0.93}$	$58.2_{2.6}$	$20.33_{0.16}$	$18.78_{0.24}$	$0.707_{0.032}$
510	$522.1_{1.7}$	$69.5_{3.4}$	$23.40_{0.28}$	$17.36_{0.25}$	$0.668_{0.034}$
520	$499.8_{2.6}$	$83.7_{3.9}$	$26.82_{0.43}$	$15.71_{0.22}$	$0.624_{0.031}$

Table SI.X: GCMC-MBAR results for the first iteration ($\theta^{\langle 1 \rangle}$) $\lambda_{\mathrm{CH_2}} = 18$ force field. Subscripts correspond to the 95% confidence interval computed with bootstrap re-sampling.

T^{sat} (K)	$\rho_{\mathrm{liq}}^{\mathrm{sat}}$ (kg/m^3)	$\rho_{\mathrm{vap}}^{\mathrm{sat}}$ (kg/m^3)	$P_{\mathrm{vap}}^{\mathrm{sat}}$ (MPa)	ΔH_{v} (kJ/mol)	$Z_{\mathrm{vap}}^{\mathrm{sat}}$
360	$713.60_{0.89}$	$3.294_{0.099}$	$1.126_{0.020}$	$30.527_{0.066}$	$0.961_{0.034}$
370	$702.86_{0.81}$	$4.306_{0.092}$	$1.499_{0.015}$	$29.921_{0.044}$	$0.952_{0.023}$
380	$692.51_{0.62}$	$5.545_{0.081}$	$1.962_{0.013}$	$29.327_{0.039}$	$0.943_{0.015}$
390	$682.23_{0.53}$	$7.043_{0.088}$	$2.529_{0.011}$	$28.725_{0.043}$	$0.932_{0.012}$
400	$671.99_{0.38}$	$8.84_{0.13}$	$3.21_{0.01}$	$28.110_{0.043}$	$0.920_{0.013}$
410	$661.74_{0.33}$	$10.98_{0.17}$	$4.029_{0.013}$	$27.478_{0.038}$	$0.906_{0.015}$
420	$650.92_{0.46}$	$13.51_{0.21}$	$4.995_{0.024}$	$26.801_{0.037}$	$0.891_{0.015}$
430	$639.09_{0.44}$	$16.48_{0.24}$	$6.125_{0.039}$	$26.056_{0.039}$	$0.875_{0.014}$
440	$626.49_{0.39}$	$19.96_{0.27}$	$7.435_{0.055}$	$25.253_{0.042}$	$0.857_{0.013}$
450	$613.53_{0.38}$	$24.02_{0.35}$	$8.941_{0.073}$	$24.409_{0.048}$	$0.837_{0.014}$
460	$600.27_{0.57}$	$28.75_{0.70}$	$10.662_{0.096}$	$23.525_{0.086}$	$0.816_{0.021}$
470	$586.50_{0.90}$	$34.3_{1.6}$	$12.62_{0.14}$	$22.58_{0.16}$	$0.793_{0.037}$
480	$571.9_{1.5}$	$40.7_{2.6}$	$14.82_{0.23}$	$21.56_{0.21}$	$0.767_{0.051}$
490	$556.3_{2.5}$	$48.4_{3.2}$	$17.30_{0.35}$	$20.44_{0.25}$	$0.738_{0.050}$
500	$538.9_{3.0}$	$57.7_{3.1}$	$20.08_{0.46}$	$19.16_{0.25}$	$0.705_{0.041}$
510	$519.1_{2.0}$	$69.1_{2.7}$	$23.19_{0.54}$	$17.67_{0.18}$	$0.666_{0.030}$
520	$495.9_{1.6}$	$83.5_{2.4}$	$26.66_{0.62}$	$15.93_{0.12}$	$0.621_{0.023}$

Table SI.XI: GCMC-MBAR results for the first iteration ($\theta^{\langle 1 \rangle}$) $\lambda_{\mathrm{CH_2}} = 20$ force field. Subscripts correspond to the 95% confidence interval computed with bootstrap re-sampling.

T^{sat} (K)	$\rho_{\mathrm{liq}}^{\mathrm{sat}}$ (kg/m^3)	$\rho_{\mathrm{vap}}^{\mathrm{sat}}$ (kg/m^3)	$P_{\mathrm{vap}}^{\mathrm{sat}}$ (MPa)	ΔH_{v} (kJ/mol)	$Z_{\mathrm{vap}}^{\mathrm{sat}}$
360	$721.21_{0.17}$	$2.885_{0.047}$	$0.989_{0.059}$	$31.72_{0.18}$	$0.964_{0.059}$
370	$711.38_{0.48}$	$3.812_{0.043}$	$1.331_{0.056}$	$31.13_{0.11}$	$0.955_{0.042}$
380	$701.58_{0.81}$	$4.955_{0.041}$	$1.759_{0.054}$	$30.545_{0.066}$	$0.946_{0.030}$
390	$691.47_{0.70}$	$6.351_{0.048}$	$2.288_{0.054}$	$29.931_{0.055}$	$0.935_{0.023}$
400	$680.14_{0.36}$	$8.033_{0.065}$	$2.932_{0.055}$	$29.243_{0.046}$	$0.924_{0.019}$
410	$668.26_{0.63}$	$10.039_{0.086}$	$3.705_{0.057}$	$28.510_{0.057}$	$0.911_{0.016}$
420	$656.5_{1.6}$	$12.41_{0.11}$	$4.621_{0.061}$	$27.77_{0.10}$	$0.897_{0.014}$
430	$644.5_{2.3}$	$15.21_{0.13}$	$5.698_{0.065}$	$27.00_{0.14}$	$0.882_{0.013}$
440	$631.8_{1.8}$	$18.50_{0.16}$	$6.950_{0.068}$	$26.17_{0.12}$	$0.864_{0.011}$
450	$618.8_{1.1}$	$22.34_{0.20}$	$8.396_{0.072}$	$25.308_{0.082}$	$0.845_{0.010}$
460	$605.44_{0.73}$	$26.84_{0.33}$	$10.053_{0.072}$	$24.399_{0.086}$	$0.824_{0.012}$
470	$591.81_{0.70}$	$32.11_{0.65}$	$11.941_{0.069}$	$23.44_{0.13}$	$0.801_{0.017}$
480	$577.60_{0.68}$	$38.3_{1.2}$	$14.083_{0.074}$	$22.41_{0.19}$	$0.775_{0.025}$
490	$562.27_{0.91}$	$45.7_{2.1}$	$16.50_{0.12}$	$21.28_{0.23}$	$0.746_{0.034}$
500	$545.2_{2.6}$	$54.6_{2.9}$	$19.22_{0.23}$	$20.00_{0.19}$	$0.713_{0.039}$
510	$526.1_{5.6}$	$65.5_{3.4}$	$22.27_{0.38}$	$18.526_{0.093}$	$0.675_{0.037}$
520	$504.1_{9.3}$	$79.2_{3.3}$	$25.69_{0.57}$	$16.81_{0.22}$	$0.631_{0.030}$

SI.V Compressibility factor

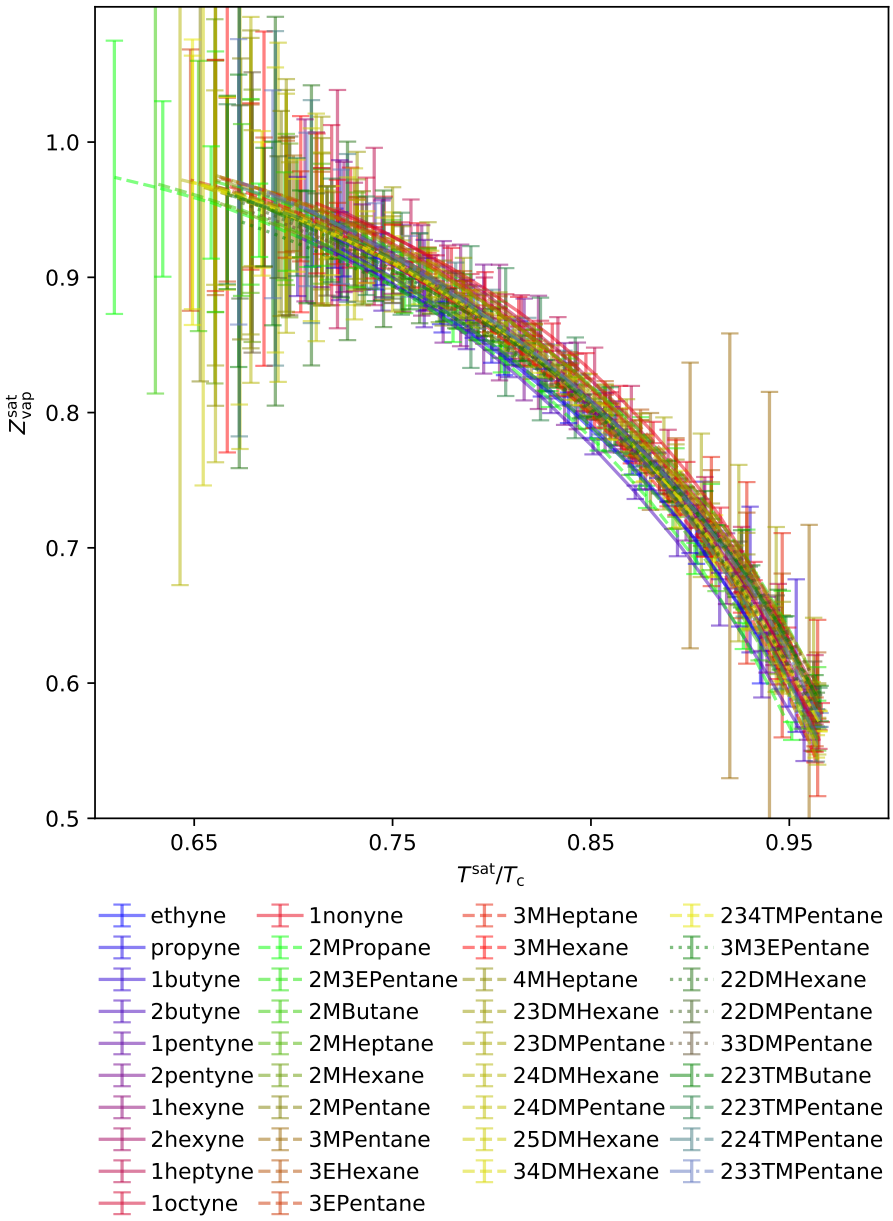

Figure SI.2: Compressibility factor in saturated vapor phase ($Z_{\text{vap}}^{\text{sat}}$) for all compounds simulated in Mick et al. and Soroush Barhaghi et al. Note that symmetric (normal) 95% confidence intervals are ill-suited when $Z_{\text{vap}}^{\text{sat}} \approx 1$, as this assumption can result in $Z_{\text{vap}}^{\text{sat}} > 1$.

SI.VI Tabulated phase equilibria for validation of GCMC-MBAR

SI.VI.1 Branched alkanes

Table SI.XII: GCMC-MBAR results for 2-methylpentane with the MiPPE-SL force field. Subscripts correspond to the 95% confidence interval computed with bootstrap re-sampling.

T^{sat} (K)	$\rho_{\mathrm{liq}}^{\mathrm{sat}}$ (kg/m^3)	$\rho_{\mathrm{vap}}^{\mathrm{sat}}$ (kg/m^3)	$P_{\mathrm{vap}}^{\mathrm{sat}}$ (MPa)	ΔH_{v} (kJ/mol)	$Z_{\mathrm{vap}}^{\mathrm{sat}}$
470	$422.20_{0.56}$	$76.7_{1.5}$	$20.68_{0.17}$	$14.14_{0.11}$	$0.595_{0.012}$
460	$444.71_{0.79}$	$61.2_{1.2}$	$17.61_{0.13}$	$16.06_{0.12}$	$0.649_{0.013}$
450	$464.38_{0.87}$	$49.31_{0.88}$	$14.918_{0.096}$	$17.71_{0.11}$	$0.697_{0.013}$
440	$481.69_{0.77}$	$40.17_{0.64}$	$12.557_{0.068}$	$19.106_{0.090}$	$0.736_{0.012}$
430	$497.34_{0.70}$	$32.86_{0.47}$	$10.491_{0.045}$	$20.318_{0.074}$	$0.770_{0.012}$
420	$511.89_{0.78}$	$26.86_{0.36}$	$8.690_{0.027}$	$21.408_{0.068}$	$0.798_{0.011}$
410	$525.69_{0.84}$	$21.87_{0.29}$	$7.130_{0.017}$	$22.412_{0.069}$	$0.824_{0.011}$
400	$538.82_{0.88}$	$17.70_{0.25}$	$5.788_{0.020}$	$23.344_{0.069}$	$0.848_{0.012}$
390	$551.23_{0.87}$	$14.21_{0.22}$	$4.645_{0.031}$	$24.207_{0.075}$	$0.869_{0.014}$
380	$562.89_{0.80}$	$11.30_{0.19}$	$3.681_{0.042}$	$25.004_{0.096}$	$0.888_{0.018}$
370	$573.96_{0.88}$	$8.90_{0.16}$	$2.878_{0.051}$	$25.75_{0.14}$	$0.906_{0.023}$
360	$584.8_{1.1}$	$6.92_{0.14}$	$2.215_{0.059}$	$26.46_{0.18}$	$0.922_{0.031}$
350	$595.6_{1.2}$	$5.31_{0.12}$	$1.677_{0.065}$	$27.15_{0.22}$	$0.935_{0.042}$
340	$606.3_{1.2}$	$4.01_{0.10}$	$1.245_{0.070}$	$27.83_{0.27}$	$0.947_{0.059}$
330	$616.4_{1.0}$	$2.969_{0.085}$	$0.906_{0.074}$	$28.45_{0.32}$	$0.958_{0.083}$
320	$625.82_{0.57}$	$2.156_{0.068}$	$0.644_{0.078}$	$29.04_{0.40}$	$0.97_{0.12}$

Table SI.XIII: GCMC-MBAR results for 2-methylhexane with the MiPPE-SL force field. Subscripts correspond to the 95% confidence interval computed with bootstrap re-sampling.

T^{sat} (K)	$\rho_{\mathrm{liq}}^{\mathrm{sat}}$ (kg/m^3)	$\rho_{\mathrm{vap}}^{\mathrm{sat}}$ (kg/m^3)	$P_{\mathrm{vap}}^{\mathrm{sat}}$ (MPa)	ΔH_{v} (kJ/mol)	$Z_{\mathrm{vap}}^{\mathrm{sat}}$
510	$406.8_{3.4}$	$88.4_{2.0}$	$20.92_{0.11}$	$14.14_{0.12}$	$0.559_{0.013}$
500	$431.2_{2.2}$	$70.0_{1.6}$	$17.989_{0.052}$	$16.506_{0.085}$	$0.620_{0.014}$
490	$452.1_{1.2}$	$56.5_{1.0}$	$15.403_{0.041}$	$18.472_{0.088}$	$0.671_{0.013}$
480	$470.38_{0.73}$	$46.30_{0.50}$	$13.120_{0.056}$	$20.092_{0.065}$	$0.7116_{8.3e-3}$
470	$486.88_{0.50}$	$38.21_{0.17}$	$11.104_{0.062}$	$21.497_{0.034}$	$0.7453_{5.3e-3}$
460	$502.20_{0.37}$	$31.56_{0.16}$	$9.327_{0.058}$	$22.762_{0.022}$	$0.7744_{6.2e-3}$
450	$516.52_{0.39}$	$26.01_{0.17}$	$7.772_{0.050}$	$23.921_{0.024}$	$0.8003_{7.3e-3}$
440	$530.01_{0.34}$	$21.34_{0.15}$	$6.417_{0.043}$	$24.994_{0.024}$	$0.8236_{7.9e-3}$
430	$542.86_{0.37}$	$17.41_{0.14}$	$5.245_{0.039}$	$25.998_{0.031}$	$0.8444_{9.1e-3}$
420	$554.93_{0.46}$	$14.10_{0.13}$	$4.241_{0.037}$	$26.928_{0.041}$	$0.863_{0.011}$
410	$566.22_{0.43}$	$11.32_{0.14}$	$3.390_{0.036}$	$27.789_{0.046}$	$0.881_{0.014}$
400	$577.21_{0.43}$	$8.99_{0.14}$	$2.674_{0.037}$	$28.610_{0.060}$	$0.896_{0.019}$
390	$588.02_{0.38}$	$7.06_{0.15}$	$2.080_{0.039}$	$29.403_{0.089}$	$0.910_{0.026}$
380	$598.35_{0.22}$	$5.47_{0.16}$	$1.593_{0.044}$	$30.15_{0.14}$	$0.923_{0.037}$
370	$608.04_{0.19}$	$4.18_{0.16}$	$1.200_{0.050}$	$30.85_{0.20}$	$0.935_{0.053}$
360	$617.49_{0.27}$	$3.14_{0.16}$	$0.888_{0.057}$	$31.52_{0.28}$	$0.945_{0.077}$
350	$627.22_{0.26}$	$2.32_{0.15}$	$0.644_{0.065}$	$32.20_{0.39}$	$0.96_{0.11}$

Table SI.XIV: GCMC-MBAR results for 3-methylpentane with the MiPPE-SL force field. Subscripts correspond to the 95% confidence interval computed with bootstrap re-sampling.

T^{sat} (K)	$\rho_{\mathrm{liq}}^{\mathrm{sat}}$ (kg/m^3)	$\rho_{\mathrm{vap}}^{\mathrm{sat}}$ (kg/m^3)	$P_{\mathrm{vap}}^{\mathrm{sat}}$ (MPa)	ΔH_{v} (kJ/mol)	$Z_{\mathrm{vap}}^{\mathrm{sat}}$
480	$415.8_{1.5}$	84_{24}	$23.1_{2.4}$	$13.7_{1.3}$	$0.60_{0.18}$
470	$440.0_{2.3}$	67_{24}	$19.9_{1.4}$	$15.6_{1.7}$	$0.65_{0.23}$
460	$459.8_{2.5}$	55_{18}	$16.98_{0.59}$	$17.2_{1.6}$	$0.69_{0.22}$
450	$477.1_{1.9}$	$45.4_{7.6}$	$14.43_{0.12}$	$18.52_{0.94}$	$0.73_{0.12}$
440	$493.2_{1.2}$	$37.5_{1.5}$	$12.17_{0.14}$	$19.74_{0.27}$	$0.764_{0.032}$
430	$508.9_{1.4}$	$30.95_{0.38}$	$10.19_{0.15}$	$20.87_{0.11}$	$0.794_{0.015}$
420	$523.6_{1.1}$	$25.42_{0.36}$	$8.45_{0.14}$	$21.917_{0.094}$	$0.821_{0.018}$
410	$536.8_{1.4}$	$20.78_{0.32}$	$6.95_{0.14}$	$22.85_{0.12}$	$0.845_{0.021}$
400	$548.9_{1.7}$	$16.89_{0.24}$	$5.65_{0.13}$	$23.69_{0.15}$	$0.867_{0.023}$
390	$560.5_{1.5}$	$13.63_{0.21}$	$4.55_{0.12}$	$24.49_{0.13}$	$0.887_{0.027}$
380	$571.8_{1.2}$	$10.88_{0.20}$	$3.61_{0.10}$	$25.250_{0.099}$	$0.905_{0.031}$
370	$582.3_{1.1}$	$8.59_{0.18}$	$2.829_{0.089}$	$25.950_{0.093}$	$0.922_{0.035}$
360	$593.0_{1.1}$	$6.70_{0.16}$	$2.185_{0.077}$	$26.64_{0.12}$	$0.939_{0.040}$
350	$603.8_{1.0}$	$5.15_{0.14}$	$1.661_{0.067}$	$27.33_{0.14}$	$0.955_{0.047}$

Table SI.XV: GCMC-MBAR results for 3-methylhexane with the MiPPE-SL force field. Subscripts correspond to the 95% confidence interval computed with bootstrap re-sampling.

T^{sat} (K)	$\rho_{\mathrm{liq}}^{\mathrm{sat}}$ (kg/m^3)	$\rho_{\mathrm{vap}}^{\mathrm{sat}}$ (kg/m^3)	$P_{\mathrm{vap}}^{\mathrm{sat}}$ (MPa)	ΔH_{v} (kJ/mol)	$Z_{\mathrm{vap}}^{\mathrm{sat}}$
520	$398.4_{4.6}$	$98.1_{1.2}$	$23.07_{0.18}$	$13.25_{0.29}$	$0.5453_{7.9e-3}$
510	$426.2_{3.4}$	$77.3_{1.3}$	$19.96_{0.15}$	$15.86_{0.21}$	$0.610_{0.011}$
500	$449.0_{1.8}$	$62.6_{1.1}$	$17.20_{0.12}$	$17.92_{0.14}$	$0.662_{0.013}$
490	$467.85_{0.87}$	$51.64_{0.76}$	$14.74_{0.11}$	$19.56_{0.10}$	$0.702_{0.011}$
480	$484.12_{0.71}$	$42.82_{0.51}$	$12.562_{0.093}$	$20.963_{0.074}$	$0.737_{0.010}$
470	$498.93_{0.76}$	$35.54_{0.44}$	$10.638_{0.075}$	$22.215_{0.069}$	$0.768_{0.011}$
460	$512.9_{1.0}$	$29.46_{0.42}$	$8.944_{0.056}$	$23.366_{0.088}$	$0.796_{0.012}$
450	$526.2_{1.3}$	$24.34_{0.36}$	$7.463_{0.040}$	$24.442_{0.093}$	$0.821_{0.013}$
440	$539.09_{0.79}$	$20.03_{0.26}$	$6.171_{0.029}$	$25.454_{0.048}$	$0.844_{0.011}$
430	$551.25_{0.90}$	$16.38_{0.15}$	$5.055_{0.025}$	$26.397_{0.089}$	$0.8648_{8.9e-3}$
420	$563.0_{1.6}$	$13.302_{0.087}$	$4.097_{0.025}$	$27.29_{0.16}$	$0.8838_{7.9e-3}$
410	$574.5_{1.4}$	$10.70_{0.12}$	$3.283_{0.024}$	$28.15_{0.18}$	$0.902_{0.012}$
400	$585.3_{1.3}$	$8.53_{0.18}$	$2.598_{0.021}$	$28.96_{0.19}$	$0.918_{0.021}$
390	$595.7_{2.4}$	$6.72_{0.26}$	$2.028_{0.021}$	$29.72_{0.30}$	$0.933_{0.037}$
380	$605.9_{2.8}$	$5.23_{0.33}$	$1.560_{0.032}$	$30.45_{0.41}$	$0.947_{0.063}$
370	$615.4_{1.3}$	$4.01_{0.38}$	$1.181_{0.053}$	$31.13_{0.47}$	$0.96_{0.10}$
360	$624.92_{0.55}$	$3.04_{0.40}$	$0.878_{0.081}$	$31.78_{0.63}$	$0.97_{0.16}$

Table SI.XVI: GCMC-MBAR results for 2,3-dimethylpentane with the MiPPE-SL force field. Subscripts correspond to the 95% confidence interval computed with bootstrap re-sampling.

T^{sat} (K)	$\rho_{\mathrm{liq}}^{\mathrm{sat}}$ (kg/m^3)	$\rho_{\mathrm{vap}}^{\mathrm{sat}}$ (kg/m^3)	$P_{\mathrm{vap}}^{\mathrm{sat}}$ (MPa)	ΔH_{v} (kJ/mol)	$Z_{\mathrm{vap}}^{\mathrm{sat}}$
510	$427.9_{1.6}$	81_{10}	$20.82_{0.91}$	$15.20_{0.53}$	$0.606_{0.081}$
500	$451.7_{1.0}$	$66.3_{9.6}$	$18.00_{0.57}$	$17.17_{0.70}$	$0.654_{0.097}$
490	$471.41_{0.86}$	$54.7_{7.1}$	$15.49_{0.28}$	$18.83_{0.70}$	$0.696_{0.091}$
480	$488.48_{0.89}$	$45.5_{4.0}$	$13.245_{0.092}$	$20.25_{0.54}$	$0.731_{0.064}$
470	$503.90_{0.73}$	$37.9_{1.7}$	$11.257_{0.050}$	$21.50_{0.32}$	$0.762_{0.035}$
460	$518.28_{0.52}$	$31.50_{0.62}$	$9.501_{0.072}$	$22.64_{0.14}$	$0.790_{0.017}$
450	$532.03_{0.63}$	$26.12_{0.25}$	$7.956_{0.080}$	$23.709_{0.054}$	$0.816_{0.011}$
440	$545.26_{0.62}$	$21.57_{0.18}$	$6.606_{0.080}$	$24.711_{0.037}$	$0.839_{0.012}$
430	$557.77_{0.54}$	$17.70_{0.16}$	$5.435_{0.075}$	$25.646_{0.038}$	$0.860_{0.014}$
420	$569.33_{0.53}$	$14.43_{0.15}$	$4.426_{0.070}$	$26.504_{0.037}$	$0.880_{0.016}$
410	$580.03_{0.59}$	$11.68_{0.14}$	$3.565_{0.063}$	$27.290_{0.040}$	$0.897_{0.019}$
400	$590.33_{0.66}$	$9.36_{0.13}$	$2.837_{0.057}$	$28.032_{0.047}$	$0.913_{0.022}$
390	$600.50_{0.61}$	$7.43_{0.11}$	$2.229_{0.052}$	$28.747_{0.057}$	$0.927_{0.026}$
380	$610.33_{0.59}$	$5.831_{0.094}$	$1.726_{0.048}$	$29.424_{0.079}$	$0.939_{0.030}$
370	$620.01_{0.64}$	$4.512_{0.077}$	$1.315_{0.046}$	$30.08_{0.11}$	$0.950_{0.037}$
360	$630.25_{0.55}$	$3.438_{0.066}$	$0.984_{0.045}$	$30.75_{0.14}$	$0.959_{0.048}$
350	$640.58_{0.49}$	$2.572_{0.058}$	$0.722_{0.046}$	$31.42_{0.20}$	$0.966_{0.065}$

Table SI.XVII: GCMC-MBAR results for 2,3-dimethylhexane with the MiPPE-SL force field. Subscripts correspond to the 95% confidence interval computed with bootstrap re-sampling.

T^{sat} (K)	$\rho_{\mathrm{liq}}^{\mathrm{sat}}$ (kg/m^3)	$\rho_{\mathrm{vap}}^{\mathrm{sat}}$ (kg/m^3)	$P_{\mathrm{vap}}^{\mathrm{sat}}$ (MPa)	ΔH_{v} (kJ/mol)	$Z_{\mathrm{vap}}^{\mathrm{sat}}$
540	$422.2_{1.1}$	$84.5_{3.7}$	$19.48_{0.48}$	$15.98_{0.12}$	$0.586_{0.029}$
530	$445.87_{0.82}$	$68.6_{3.6}$	$16.89_{0.36}$	$18.23_{0.22}$	$0.638_{0.036}$
520	$466.30_{0.66}$	$56.3_{3.0}$	$14.58_{0.24}$	$20.17_{0.26}$	$0.684_{0.038}$
510	$484.13_{0.59}$	$46.7_{2.1}$	$12.53_{0.15}$	$21.81_{0.23}$	$0.722_{0.034}$
500	$499.99_{0.52}$	$39.0_{1.4}$	$10.703_{0.092}$	$23.24_{0.18}$	$0.755_{0.027}$
490	$514.34_{0.48}$	$32.51_{0.80}$	$9.084_{0.054}$	$24.51_{0.13}$	$0.783_{0.020}$
480	$527.67_{0.54}$	$27.08_{0.47}$	$7.657_{0.032}$	$25.677_{0.096}$	$0.809_{0.014}$
470	$540.41_{0.64}$	$22.49_{0.30}$	$6.406_{0.019}$	$26.765_{0.082}$	$0.833_{0.012}$
460	$552.77_{0.76}$	$18.58_{0.23}$	$5.313_{0.015}$	$27.797_{0.085}$	$0.854_{0.011}$
450	$564.84_{0.87}$	$15.26_{0.22}$	$4.366_{0.018}$	$28.78_{0.11}$	$0.874_{0.013}$
440	$576.56_{0.95}$	$12.43_{0.23}$	$3.553_{0.025}$	$29.73_{0.14}$	$0.892_{0.017}$
430	$587.55_{0.97}$	$10.05_{0.23}$	$2.860_{0.034}$	$30.60_{0.18}$	$0.909_{0.023}$
420	$597.72_{0.83}$	$8.05_{0.21}$	$2.274_{0.044}$	$31.40_{0.21}$	$0.924_{0.030}$
410	$607.46_{0.53}$	$6.39_{0.18}$	$1.787_{0.053}$	$32.16_{0.22}$	$0.937_{0.038}$
400	$617.12_{0.48}$	$5.01_{0.14}$	$1.384_{0.061}$	$32.90_{0.24}$	$0.949_{0.050}$
390	$626.72_{0.62}$	$3.88_{0.10}$	$1.056_{0.067}$	$33.64_{0.28}$	$0.959_{0.066}$
380	$636.43_{0.54}$	$2.959_{0.070}$	$0.792_{0.071}$	$34.36_{0.35}$	$0.967_{0.090}$
370	$646.47_{0.59}$	$2.219_{0.049}$	$0.583_{0.072}$	$35.10_{0.46}$	$0.98_{0.12}$

Table SI.XVIII: GCMC-MBAR results for 2,4-dimethylhexane with the MiPPE-SL force field. Subscripts correspond to the 95% confidence interval computed with bootstrap resampling.

T^{sat} (K)	$\rho_{\mathrm{liq}}^{\mathrm{sat}}$ (kg/m^3)	$\rho_{\mathrm{vap}}^{\mathrm{sat}}$ (kg/m^3)	$P_{\mathrm{vap}}^{\mathrm{sat}}$ (MPa)	ΔH_{v} (kJ/mol)	$Z_{\mathrm{vap}}^{\mathrm{sat}}$
540	$406.0_{3.8}$	$97.8_{2.1}$	$20.90_{0.36}$	$14.21_{0.22}$	$0.543_{0.015}$
530	$430.3_{3.2}$	$78.1_{2.3}$	$18.10_{0.28}$	$16.71_{0.16}$	$0.601_{0.020}$
520	$452.1_{1.9}$	$63.1_{2.2}$	$15.62_{0.19}$	$18.90_{0.15}$	$0.654_{0.024}$
510	$470.9_{1.1}$	$51.8_{1.9}$	$13.42_{0.13}$	$20.72_{0.19}$	$0.698_{0.026}$
500	$487.5_{1.1}$	$42.9_{1.4}$	$11.472_{0.080}$	$22.26_{0.19}$	$0.734_{0.024}$
490	$502.5_{1.2}$	$35.72_{0.85}$	$9.745_{0.054}$	$23.60_{0.16}$	$0.765_{0.019}$
480	$516.3_{1.4}$	$29.69_{0.47}$	$8.222_{0.043}$	$24.83_{0.13}$	$0.793_{0.013}$
470	$529.5_{1.6}$	$24.62_{0.27}$	$6.886_{0.037}$	$25.96_{0.11}$	$0.8174_{9.9e-3}$
460	$542.1_{1.7}$	$20.34_{0.18}$	$5.720_{0.031}$	$27.026_{0.098}$	$0.8399_{8.6e-3}$
450	$554.3_{1.8}$	$16.71_{0.13}$	$4.708_{0.026}$	$28.031_{0.098}$	$0.8603_{8.3e-3}$
440	$566.1_{1.8}$	$13.63_{0.10}$	$3.836_{0.024}$	$28.98_{0.10}$	$0.8786_{8.6e-3}$
430	$577.4_{1.6}$	$11.03_{0.11}$	$3.092_{0.023}$	$29.89_{0.11}$	$0.895_{0.011}$
420	$588.1_{1.4}$	$8.85_{0.15}$	$2.463_{0.022}$	$30.73_{0.13}$	$0.910_{0.018}$
410	$598.1_{1.1}$	$7.02_{0.19}$	$1.937_{0.024}$	$31.51_{0.17}$	$0.924_{0.028}$
400	$607.97_{0.72}$	$5.51_{0.22}$	$1.503_{0.031}$	$32.27_{0.22}$	$0.937_{0.042}$
390	$617.69_{0.31}$	$4.27_{0.23}$	$1.148_{0.042}$	$33.01_{0.29}$	$0.947_{0.062}$
380	$627.04_{0.22}$	$3.26_{0.22}$	$0.862_{0.055}$	$33.71_{0.42}$	$0.957_{0.090}$
370	$635.81_{0.19}$	$2.45_{0.20}$	$0.636_{0.068}$	$34.36_{0.62}$	$0.97_{0.13}$
360	$644.04_{0.32}$	$1.80_{0.18}$	$0.460_{0.080}$	$34.97_{0.91}$	$0.97_{0.19}$

Table SI.XIX: GCMC-MBAR results for 3,4-dimethylhexane with the MiPPE-SL force field. Subscripts correspond to the 95% confidence interval computed with bootstrap re-sampling.

T^{sat} (K)	$\rho_{\mathrm{liq}}^{\mathrm{sat}}$ (kg/m^3)	$\rho_{\mathrm{vap}}^{\mathrm{sat}}$ (kg/m^3)	$P_{\mathrm{vap}}^{\mathrm{sat}}$ (MPa)	ΔH_{v} (kJ/mol)	$Z_{\mathrm{vap}}^{\mathrm{sat}}$
550	$416.97_{0.84}$	$91.7_{2.1}$	$21.00_{0.24}$	$15.29_{0.11}$	$0.572_{0.015}$
540	$441.75_{0.84}$	$75.2_{2.0}$	$18.28_{0.18}$	$17.53_{0.13}$	$0.619_{0.017}$
530	$462.97_{0.65}$	$61.9_{1.6}$	$15.84_{0.12}$	$19.50_{0.14}$	$0.664_{0.018}$
520	$481.27_{0.52}$	$51.4_{1.2}$	$13.670_{0.076}$	$21.20_{0.13}$	$0.703_{0.017}$
510	$497.59_{0.51}$	$42.88_{0.80}$	$11.732_{0.044}$	$22.68_{0.12}$	$0.737_{0.014}$
500	$512.45_{0.50}$	$35.87_{0.49}$	$10.010_{0.025}$	$23.994_{0.090}$	$0.767_{0.011}$
490	$526.21_{0.55}$	$30.00_{0.31}$	$8.485_{0.015}$	$25.192_{0.073}$	$0.7931_{8.3e-3}$
480	$539.20_{0.79}$	$25.02_{0.22}$	$7.142_{0.014}$	$26.302_{0.072}$	$0.8169_{7.4e-3}$
470	$551.6_{1.1}$	$20.79_{0.18}$	$5.963_{0.017}$	$27.341_{0.083}$	$0.8385_{7.6e-3}$
460	$563.5_{1.3}$	$17.18_{0.15}$	$4.936_{0.023}$	$28.319_{0.097}$	$0.8583_{8.7e-3}$
450	$574.7_{1.3}$	$14.10_{0.14}$	$4.050_{0.028}$	$29.24_{0.11}$	$0.877_{0.011}$
440	$585.4_{1.2}$	$11.49_{0.12}$	$3.287_{0.033}$	$30.09_{0.11}$	$0.893_{0.013}$
430	$595.6_{1.1}$	$9.29_{0.11}$	$2.642_{0.037}$	$30.90_{0.11}$	$0.909_{0.017}$
420	$605.36_{0.91}$	$7.437_{0.097}$	$2.097_{0.040}$	$31.66_{0.11}$	$0.922_{0.021}$
410	$614.74_{0.65}$	$5.893_{0.085}$	$1.644_{0.042}$	$32.38_{0.12}$	$0.935_{0.027}$
400	$624.02_{0.41}$	$4.615_{0.075}$	$1.271_{0.044}$	$33.08_{0.14}$	$0.946_{0.036}$
390	$633.41_{0.31}$	$3.566_{0.067}$	$0.967_{0.045}$	$33.78_{0.17}$	$0.955_{0.048}$
380	$642.95_{0.22}$	$2.715_{0.059}$	$0.724_{0.045}$	$34.48_{0.22}$	$0.964_{0.064}$
370	$652.67_{0.19}$	$2.032_{0.051}$	$0.531_{0.046}$	$35.18_{0.29}$	$0.970_{0.087}$

Table SI.XX: GCMC-MBAR results for 2,2,3-trimethylbutane with the MiPPE-SL force field. Subscripts correspond to the 95% confidence interval computed with bootstrap re-sampling.

T^{sat} (K)	$\rho_{\mathrm{liq}}^{\mathrm{sat}}$ (kg/m^3)	$\rho_{\mathrm{vap}}^{\mathrm{sat}}$ (kg/m^3)	$P_{\mathrm{vap}}^{\mathrm{sat}}$ (MPa)	ΔH_{v} (kJ/mol)	$Z_{\mathrm{vap}}^{\mathrm{sat}}$
520	$427.6_{2.7}$	$90.4_{3.4}$	$23.10_{0.41}$	$14.20_{0.20}$	$0.592_{0.025}$
510	$451.1_{1.5}$	$73.9_{3.6}$	$20.14_{0.30}$	$16.22_{0.27}$	$0.644_{0.033}$
500	$471.00_{0.92}$	$61.5_{2.9}$	$17.48_{0.20}$	$17.84_{0.29}$	$0.684_{0.033}$
490	$488.37_{0.82}$	$51.6_{1.9}$	$15.09_{0.14}$	$19.22_{0.23}$	$0.719_{0.027}$
480	$503.84_{0.76}$	$43.39_{0.99}$	$12.95_{0.11}$	$20.44_{0.15}$	$0.749_{0.018}$
470	$518.11_{0.61}$	$36.42_{0.54}$	$11.046_{0.087}$	$21.544_{0.083}$	$0.778_{0.013}$
460	$531.60_{0.50}$	$30.51_{0.45}$	$9.358_{0.068}$	$22.566_{0.064}$	$0.803_{0.013}$
450	$544.35_{0.55}$	$25.49_{0.41}$	$7.870_{0.049}$	$23.512_{0.070}$	$0.827_{0.014}$
440	$556.68_{0.54}$	$21.21_{0.32}$	$6.564_{0.032}$	$24.402_{0.069}$	$0.848_{0.014}$
430	$568.85_{0.50}$	$17.55_{0.23}$	$5.424_{0.020}$	$25.255_{0.062}$	$0.866_{0.012}$
420	$580.37_{0.55}$	$14.42_{0.15}$	$4.436_{0.014}$	$26.050_{0.058}$	$0.8826_{9.3e-3}$
410	$590.79_{0.86}$	$11.748_{0.088}$	$3.590_{0.014}$	$26.769_{0.064}$	$0.8982_{7.5e-3}$
400	$600.6_{1.0}$	$9.476_{0.069}$	$2.870_{0.014}$	$27.440_{0.077}$	$0.9126_{8.0e-3}$
390	$610.62_{0.83}$	$7.560_{0.096}$	$2.267_{0.013}$	$28.107_{0.086}$	$0.927_{0.013}$
380	$621.8_{1.5}$	$5.96_{0.14}$	$1.765_{0.014}$	$28.82_{0.16}$	$0.940_{0.023}$
370	$633.5_{2.1}$	$4.63_{0.17}$	$1.353_{0.019}$	$29.56_{0.26}$	$0.952_{0.038}$
360	$643.07_{0.71}$	$3.54_{0.20}$	$1.019_{0.029}$	$30.16_{0.26}$	$0.963_{0.060}$

Table SI.XXI: GCMC-MBAR results for 2,2,3-trimethylpentane with the MiPPE-SL force field. Subscripts correspond to the 95% confidence interval computed with bootstrap resampling.

T^{sat} (K)	$\rho_{\mathrm{liq}}^{\mathrm{sat}}$ (kg/m^3)	$\rho_{\mathrm{vap}}^{\mathrm{sat}}$ (kg/m^3)	$P_{\mathrm{vap}}^{\mathrm{sat}}$ (MPa)	ΔH_{v} (kJ/mol)	$Z_{\mathrm{vap}}^{\mathrm{sat}}$
550	$424.5_{1.7}$	$94.6_{5.8}$	$22.04_{0.85}$	$14.90_{0.26}$	$0.582_{0.042}$
540	$446.63_{0.90}$	$77.5_{4.4}$	$19.31_{0.70}$	$17.04_{0.27}$	$0.634_{0.043}$
530	$466.95_{0.61}$	$64.6_{2.9}$	$16.85_{0.58}$	$18.86_{0.22}$	$0.676_{0.039}$
520	$485.81_{0.76}$	$54.4_{1.9}$	$14.63_{0.50}$	$20.45_{0.13}$	$0.711_{0.035}$
510	$502.62_{0.63}$	$45.9_{1.6}$	$12.63_{0.44}$	$21.840_{0.082}$	$0.742_{0.037}$
500	$517.03_{0.59}$	$38.7_{1.7}$	$10.84_{0.37}$	$23.05_{0.11}$	$0.770_{0.043}$
490	$529.98_{0.76}$	$32.6_{1.9}$	$9.25_{0.29}$	$24.14_{0.18}$	$0.795_{0.053}$
480	$542.7_{1.0}$	$27.4_{1.8}$	$7.84_{0.21}$	$25.18_{0.25}$	$0.818_{0.059}$
470	$555.2_{1.2}$	$23.0_{1.6}$	$6.59_{0.13}$	$26.17_{0.29}$	$0.840_{0.059}$
460	$566.7_{1.3}$	$19.1_{1.2}$	$5.500_{0.068}$	$27.09_{0.30}$	$0.860_{0.054}$
450	$577.6_{1.2}$	$15.82_{0.81}$	$4.550_{0.027}$	$27.94_{0.29}$	$0.878_{0.045}$
440	$588.5_{3.8}$	$13.0_{1.5}$	4_{13}	$28.8_{7.3}$	$0.9_{3.1}$
430	$599.6_{2.4}$	$10.61_{0.31}$	$3.023_{0.035}$	$29.58_{0.30}$	$0.910_{0.029}$
420	$610.1_{2.1}$	$8.58_{0.19}$	$2.423_{0.044}$	$30.34_{0.26}$	$0.923_{0.026}$
410	$619.5_{1.4}$	$6.88_{0.12}$	$1.918_{0.049}$	$31.02_{0.22}$	$0.935_{0.029}$
400	$628.4_{1.5}$	$5.447_{0.098}$	$1.498_{0.051}$	$31.66_{0.24}$	$0.945_{0.036}$
380	$645.33_{0.68}$	$3.285_{0.097}$	$0.874_{0.051}$	$32.86_{0.25}$	$0.961_{0.062}$

Table SI.XXII: GCMC-MBAR results for 2,2,4-trimethylpentane with the MiPPE-SL force field. Subscripts correspond to the 95% confidence interval computed with bootstrap resampling.

T^{sat} (K)	$\rho_{\mathrm{liq}}^{\mathrm{sat}}$ (kg/m^3)	$\rho_{\mathrm{vap}}^{\mathrm{sat}}$ (kg/m^3)	$P_{\mathrm{vap}}^{\mathrm{sat}}$ (MPa)	ΔH_{v} (kJ/mol)	$Z_{\mathrm{vap}}^{\mathrm{sat}}$
530	$400.9_{2.2}$	$97.9_{4.8}$	$21.20_{0.38}$	$13.58_{0.32}$	$0.561_{0.029}$
520	$427.5_{1.3}$	$79.4_{3.2}$	$18.44_{0.28}$	$15.89_{0.27}$	$0.614_{0.027}$
510	$448.78_{0.77}$	$65.1_{1.8}$	$15.97_{0.21}$	$17.79_{0.18}$	$0.661_{0.020}$
500	$466.83_{0.75}$	$53.9_{1.1}$	$13.78_{0.18}$	$19.40_{0.13}$	$0.702_{0.017}$
490	$483.78_{0.81}$	$44.87_{0.89}$	$11.82_{0.15}$	$20.85_{0.12}$	$0.739_{0.017}$
480	$499.84_{0.70}$	$37.41_{0.89}$	$10.09_{0.12}$	$22.18_{0.12}$	$0.772_{0.020}$
470	$514.41_{0.57}$	$31.21_{0.86}$	$8.545_{0.083}$	$23.38_{0.13}$	$0.800_{0.023}$
460	$527.62_{0.53}$	$26.00_{0.75}$	$7.187_{0.053}$	$24.45_{0.13}$	$0.826_{0.025}$
450	$539.75_{0.68}$	$21.58_{0.59}$	$5.995_{0.030}$	$25.42_{0.12}$	$0.848_{0.024}$
440	$551.12_{0.66}$	$17.82_{0.43}$	$4.958_{0.022}$	$26.32_{0.12}$	$0.869_{0.021}$
430	$562.67_{0.50}$	$14.62_{0.31}$	$4.062_{0.027}$	$27.21_{0.13}$	$0.888_{0.020}$
420	$574.59_{0.49}$	$11.89_{0.25}$	$3.292_{0.035}$	$28.09_{0.13}$	$0.906_{0.021}$
410	$585.04_{0.41}$	$9.58_{0.25}$	$2.637_{0.042}$	$28.86_{0.15}$	$0.922_{0.028}$
400	$594.23_{0.30}$	$7.66_{0.27}$	$2.087_{0.051}$	$29.54_{0.20}$	$0.936_{0.040}$
390	$604.33_{0.26}$	$6.05_{0.29}$	$1.630_{0.063}$	$30.26_{0.28}$	$0.949_{0.058}$
380	$615.43_{0.23}$	$4.72_{0.30}$	$1.252_{0.077}$	$31.01_{0.41}$	$0.958_{0.084}$
370	$625.27_{0.23}$	$3.63_{0.29}$	$0.946_{0.092}$	$31.68_{0.58}$	$0.97_{0.12}$

Table SI.XXIII: GCMC-MBAR results for 2,3,3-trimethylpentane with the MiPPE-SL force field. Subscripts correspond to the 95% confidence interval computed with bootstrap resampling.

T^{sat} (K)	$\rho_{\mathrm{liq}}^{\mathrm{sat}}$ (kg/m^3)	$\rho_{\mathrm{vap}}^{\mathrm{sat}}$ (kg/m^3)	$P_{\mathrm{vap}}^{\mathrm{sat}}$ (MPa)	ΔH_{v} (kJ/mol)	$Z_{\mathrm{vap}}^{\mathrm{sat}}$
560	$426.5_{9.5}$	$98.7_{1.6}$	$23.04_{0.24}$	$14.76_{0.51}$	$0.573_{0.011}$
550	$452.4_{5.9}$	$80.7_{1.4}$	$20.23_{0.20}$	$17.10_{0.29}$	$0.626_{0.013}$
540	$473.3_{2.0}$	$67.2_{1.1}$	$17.69_{0.18}$	$18.98_{0.12}$	$0.670_{0.013}$
530	$490.60_{0.59}$	$56.53_{0.74}$	$15.40_{0.16}$	$20.523_{0.065}$	$0.706_{0.012}$
520	$505.89_{0.92}$	$47.80_{0.63}$	$13.35_{0.14}$	$21.863_{0.043}$	$0.738_{0.012}$
510	$520.2_{1.1}$	$40.46_{0.65}$	$11.51_{0.12}$	$23.086_{0.038}$	$0.766_{0.014}$
500	$534.1_{1.0}$	$34.21_{0.66}$	$9.866_{0.088}$	$24.232_{0.057}$	$0.792_{0.017}$
490	$546.97_{0.93}$	$28.87_{0.60}$	$8.402_{0.063}$	$25.283_{0.071}$	$0.816_{0.018}$
480	$558.82_{0.80}$	$24.29_{0.47}$	$7.108_{0.044}$	$26.241_{0.071}$	$0.837_{0.017}$
470	$570.25_{0.87}$	$20.36_{0.30}$	$5.967_{0.036}$	$27.143_{0.070}$	$0.857_{0.014}$
460	$581.5_{1.1}$	$16.96_{0.17}$	$4.969_{0.037}$	$28.007_{0.066}$	$0.875_{0.011}$
450	$592.0_{1.0}$	$14.04_{0.13}$	$4.101_{0.041}$	$28.816_{0.071}$	$0.892_{0.012}$
440	$602.0_{1.1}$	$11.53_{0.15}$	$3.353_{0.046}$	$29.578_{0.085}$	$0.908_{0.017}$
430	$612.3_{1.6}$	$9.39_{0.16}$	$2.714_{0.052}$	$30.34_{0.10}$	$0.924_{0.024}$
420	$622.8_{1.6}$	$7.58_{0.16}$	$2.171_{0.058}$	$31.10_{0.13}$	$0.937_{0.032}$
410	$632.87_{0.75}$	$6.05_{0.16}$	$1.716_{0.064}$	$31.82_{0.20}$	$0.950_{0.044}$
400	$642.39_{0.29}$	$4.78_{0.17}$	$1.338_{0.070}$	$32.50_{0.28}$	$0.961_{0.061}$
390	$651.59_{0.31}$	$3.73_{0.18}$	$1.028_{0.075}$	$33.14_{0.37}$	$0.971_{0.085}$

SI.VI.2 Alkynes

Table SI.XXIV: GCMC-MBAR results for ethyne with the MiPPE force field. Subscripts correspond to the 95% confidence interval computed with bootstrap re-sampling.

T^{sat} (K)	$\rho_{\mathrm{liq}}^{\mathrm{sat}}$ (kg/m^3)	$\rho_{\mathrm{vap}}^{\mathrm{sat}}$ (kg/m^3)	$P_{\mathrm{vap}}^{\mathrm{sat}}$ (MPa)	ΔH_{v} (kJ/mol)	$Z_{\mathrm{vap}}^{\mathrm{sat}}$
290	$421.3_{3.5}$	$69.7_{3.3}$	$40.83_{0.20}$	$8.80_{0.21}$	$0.632_{0.030}$
280	$450.7_{1.9}$	$50.69_{0.91}$	$31.96_{0.26}$	$10.27_{0.12}$	$0.705_{0.014}$
270	$474.9_{3.0}$	$37.66_{0.39}$	$24.65_{0.24}$	$11.390_{0.086}$	$0.759_{0.011}$
260	$497.3_{1.1}$	$27.95_{0.53}$	$18.65_{0.17}$	$12.361_{0.034}$	$0.804_{0.017}$
250	$517.91_{0.59}$	$20.53_{0.34}$	$13.78_{0.12}$	$13.214_{0.042}$	$0.841_{0.016}$
240	$536.87_{0.67}$	$14.82_{0.12}$	$9.92_{0.10}$	$13.975_{0.028}$	$0.874_{0.011}$
230	$554.12_{0.54}$	$10.447_{0.095}$	$6.925_{0.089}$	$14.649_{0.037}$	$0.903_{0.014}$
220	$570.90_{0.53}$	$7.155_{0.097}$	$4.667_{0.082}$	$15.283_{0.049}$	$0.929_{0.021}$

Table SI.XXV: GCMC-MBAR results for propyne with the MiPPE force field. Subscripts correspond to the 95% confidence interval computed with bootstrap re-sampling.

T^{sat} (K)	$\rho_{\mathrm{liq}}^{\mathrm{sat}}$ (kg/m^3)	$\rho_{\mathrm{vap}}^{\mathrm{sat}}$ (kg/m^3)	$P_{\mathrm{vap}}^{\mathrm{sat}}$ (MPa)	ΔH_{v} (kJ/mol)	$Z_{\mathrm{vap}}^{\mathrm{sat}}$
380	$441.0_{7.9}$	$82.2_{3.1}$	$38.39_{0.90}$	$10.96_{0.34}$	$0.592_{0.026}$
370	$472.7_{5.0}$	$62.7_{2.7}$	$31.64_{0.73}$	$12.83_{0.31}$	$0.657_{0.033}$
360	$498.3_{2.8}$	$48.6_{1.9}$	$25.84_{0.57}$	$14.34_{0.24}$	$0.711_{0.032}$
350	$520.1_{2.4}$	$38.1_{1.3}$	$20.88_{0.45}$	$15.58_{0.19}$	$0.754_{0.030}$
340	$539.4_{2.1}$	$29.88_{0.90}$	$16.67_{0.35}$	$16.65_{0.15}$	$0.791_{0.029}$
330	$556.6_{1.4}$	$23.31_{0.72}$	$13.13_{0.27}$	$17.58_{0.11}$	$0.822_{0.031}$
320	$572.1_{1.3}$	$18.02_{0.60}$	$10.18_{0.19}$	$18.41_{0.11}$	$0.850_{0.032}$
310	$587.6_{1.3}$	$13.76_{0.47}$	$7.76_{0.12}$	$19.20_{0.12}$	$0.876_{0.033}$
300	$603.3_{1.5}$	$10.35_{0.32}$	$5.799_{0.068}$	$19.97_{0.13}$	$0.900_{0.030}$
290	$617.9_{2.2}$	$7.65_{0.20}$	$4.240_{0.040}$	$20.67_{0.15}$	$0.921_{0.025}$

Table SI.XXVI: GCMC-MBAR results for 1-butyne with the MiPPE force field. Subscripts correspond to the 95% confidence interval computed with bootstrap re-sampling.

T^{sat} (K)	$\rho_{\mathrm{liq}}^{\mathrm{sat}}$ (kg/m^3)	$\rho_{\mathrm{vap}}^{\mathrm{sat}}$ (kg/m^3)	$P_{\mathrm{vap}}^{\mathrm{sat}}$ (MPa)	ΔH_{v} (kJ/mol)	$Z_{\mathrm{vap}}^{\mathrm{sat}}$
410	$445.1_{5.3}$	76_{12}	$29.5_{1.0}$	$12.82_{0.72}$	$0.620_{0.097}$
400	$472.3_{3.4}$	$59.2_{6.8}$	$24.64_{0.50}$	$14.61_{0.60}$	$0.677_{0.079}$
390	$495.0_{2.6}$	$47.1_{2.3}$	$20.38_{0.30}$	$16.08_{0.32}$	$0.722_{0.037}$
380	$515.5_{2.0}$	$37.54_{0.86}$	$16.69_{0.23}$	$17.37_{0.16}$	$0.761_{0.020}$
370	$534.5_{1.3}$	$29.90_{0.70}$	$13.51_{0.18}$	$18.53_{0.13}$	$0.795_{0.021}$
360	$552.0_{1.6}$	$23.69_{0.62}$	$10.81_{0.13}$	$19.57_{0.16}$	$0.824_{0.024}$
350	$567.8_{1.9}$	$18.62_{0.51}$	$8.524_{0.086}$	$20.50_{0.18}$	$0.851_{0.025}$
340	$582.2_{1.1}$	$14.49_{0.38}$	$6.623_{0.060}$	$21.34_{0.13}$	$0.874_{0.024}$
330	$595.8_{1.1}$	$11.15_{0.24}$	$5.061_{0.049}$	$22.112_{0.082}$	$0.895_{0.021}$
320	$610.6_{2.8}$	$8.45_{0.14}$	$3.795_{0.049}$	$22.905_{0.095}$	$0.913_{0.019}$
310	$624.6_{1.8}$	$6.284_{0.087}$	$2.782_{0.051}$	$23.650_{0.059}$	$0.929_{0.021}$

Table SI.XXVII: GCMC-MBAR results for 2-butyne with the MiPPE force field. Subscripts correspond to the 95% confidence interval computed with bootstrap re-sampling.

T^{sat} (K)	$\rho_{\mathrm{liq}}^{\mathrm{sat}}$ (kg/m^3)	$\rho_{\mathrm{vap}}^{\mathrm{sat}}$ (kg/m^3)	$P_{\mathrm{vap}}^{\mathrm{sat}}$ (MPa)	ΔH_{v} (kJ/mol)	$Z_{\mathrm{vap}}^{\mathrm{sat}}$
450	$431.8_{7.4}$	$93.5_{4.3}$	$36.24_{0.50}$	$11.93_{0.26}$	$0.561_{0.027}$
440	$466.0_{5.5}$	$74.1_{3.5}$	$30.73_{0.28}$	$14.00_{0.24}$	$0.613_{0.029}$
430	$491.6_{2.0}$	$59.1_{1.9}$	$25.87_{0.16}$	$15.71_{0.17}$	$0.662_{0.022}$
420	$512.10_{0.77}$	$47.58_{0.69}$	$21.63_{0.14}$	$17.114_{0.094}$	$0.704_{0.011}$
410	$530.5_{1.1}$	$38.42_{0.30}$	$17.95_{0.13}$	$18.346_{0.054}$	$0.74_{0.01}$
400	$548.28_{0.94}$	$30.99_{0.31}$	$14.76_{0.11}$	$19.487_{0.051}$	$0.77_{0.01}$
390	$565.05_{0.94}$	$24.89_{0.27}$	$12.013_{0.089}$	$20.533_{0.061}$	$0.805_{0.011}$
380	$580.6_{1.1}$	$19.89_{0.25}$	$9.674_{0.068}$	$21.483_{0.073}$	$0.833_{0.012}$
370	$594.97_{0.83}$	$15.78_{0.25}$	$7.697_{0.050}$	$22.349_{0.074}$	$0.858_{0.014}$
360	$608.65_{0.59}$	$12.41_{0.22}$	$6.041_{0.038}$	$23.157_{0.070}$	$0.880_{0.017}$
350	$621.69_{0.66}$	$9.66_{0.19}$	$4.672_{0.041}$	$23.912_{0.091}$	$0.899_{0.019}$
340	$633.85_{0.59}$	$7.42_{0.16}$	$3.552_{0.052}$	$24.60_{0.12}$	$0.916_{0.024}$
330	$646.13_{0.73}$	$5.62_{0.13}$	$2.651_{0.064}$	$25.26_{0.16}$	$0.930_{0.031}$

Table SI.XXVIII: GCMC-MBAR results for 1-pentyne with the MiPPE force field. Subscripts correspond to the 95% confidence interval computed with bootstrap re-sampling.

T^{sat} (K)	$\rho_{\mathrm{liq}}^{\mathrm{sat}}$ (kg/m^3)	$\rho_{\mathrm{vap}}^{\mathrm{sat}}$ (kg/m^3)	$P_{\mathrm{vap}}^{\mathrm{sat}}$ (MPa)	ΔH_{v} (kJ/mol)	$Z_{\mathrm{vap}}^{\mathrm{sat}}$
450	$433.7_{2.3}$	$85.6_{2.5}$	$27.32_{0.22}$	$13.15_{0.18}$	$0.581_{0.018}$
440	$461.7_{1.7}$	$66.9_{2.0}$	$23.04_{0.15}$	$15.29_{0.18}$	$0.641_{0.020}$
430	$485.2_{1.5}$	$53.1_{1.2}$	$19.32_{0.12}$	$17.06_{0.16}$	$0.693_{0.016}$
420	$505.4_{1.6}$	$42.65_{0.51}$	$16.08_{0.12}$	$18.54_{0.11}$	$0.735_{0.010}$
410	$523.3_{1.4}$	$34.37_{0.30}$	$13.27_{0.10}$	$19.810_{0.078}$	$0.77_{0.01}$
400	$539.7_{1.2}$	$27.67_{0.31}$	$10.844_{0.077}$	$20.949_{0.055}$	$0.803_{0.011}$
390	$555.3_{1.1}$	$22.17_{0.30}$	$8.770_{0.052}$	$21.998_{0.041}$	$0.831_{0.012}$
380	$570.2_{1.0}$	$17.64_{0.27}$	$7.009_{0.033}$	$22.977_{0.033}$	$0.857_{0.014}$
370	$584.03_{0.90}$	$13.91_{0.25}$	$5.528_{0.028}$	$23.874_{0.050}$	$0.880_{0.016}$
360	$596.86_{0.83}$	$10.86_{0.22}$	$4.300_{0.040}$	$24.697_{0.083}$	$0.901_{0.020}$
350	$609.71_{0.69}$	$8.37_{0.19}$	$3.291_{0.055}$	$25.49_{0.11}$	$0.920_{0.026}$
340	$622.58_{0.99}$	$6.37_{0.15}$	$2.474_{0.070}$	$26.27_{0.13}$	$0.936_{0.035}$

Table SI.XXIX: GCMC-MBAR results for 2-pentyne with the MiPPE force field. Subscripts correspond to the 95% confidence interval computed with bootstrap re-sampling.

T^{sat} (K)	$\rho_{\mathrm{liq}}^{\mathrm{sat}}$ (kg/m^3)	$\rho_{\mathrm{vap}}^{\mathrm{sat}}$ (kg/m^3)	$P_{\mathrm{vap}}^{\mathrm{sat}}$ (MPa)	ΔH_{v} (kJ/mol)	$Z_{\mathrm{vap}}^{\mathrm{sat}}$
470	$445.8_{3.1}$	$83.4_{6.2}$	$27.7_{1.2}$	$14.09_{0.22}$	$0.578_{0.049}$
460	$473.8_{1.9}$	$65.6_{5.4}$	$23.43_{0.88}$	$16.27_{0.30}$	$0.636_{0.057}$
450	$496.8_{1.0}$	$52.5_{3.7}$	$19.73_{0.64}$	$18.06_{0.28}$	$0.685_{0.053}$
440	$516.64_{0.73}$	$42.4_{2.3}$	$16.50_{0.48}$	$19.56_{0.22}$	$0.725_{0.045}$
430	$534.83_{0.74}$	$34.3_{1.7}$	$13.69_{0.36}$	$20.89_{0.19}$	$0.761_{0.042}$
420	$551.57_{0.81}$	$27.7_{1.4}$	$11.26_{0.25}$	$22.08_{0.19}$	$0.792_{0.044}$
410	$566.89_{0.86}$	$22.3_{1.2}$	$9.17_{0.16}$	$23.16_{0.22}$	$0.821_{0.048}$
400	$581.3_{1.1}$	$17.9_{1.0}$	$7.394_{0.080}$	$24.15_{0.26}$	$0.847_{0.049}$
390	$595.3_{1.6}$	$14.24_{0.71}$	$5.890_{0.039}$	$25.09_{0.28}$	$0.869_{0.043}$
380	$608.6_{1.7}$	$11.23_{0.40}$	$4.631_{0.052}$	$25.95_{0.25}$	$0.889_{0.034}$
370	$621.0_{1.3}$	$8.76_{0.19}$	$3.587_{0.066}$	$26.75_{0.19}$	$0.907_{0.026}$
360	$632.99_{0.96}$	$6.75_{0.16}$	$2.735_{0.069}$	$27.52_{0.12}$	$0.922_{0.031}$
350	$644.7_{1.0}$	$5.12_{0.20}$	$2.049_{0.065}$	$28.249_{0.10}$	$0.937_{0.047}$

Table SI.XXX: GCMC-MBAR results for 1-hexyne with the MiPPE force field. Subscripts correspond to the 95% confidence interval computed with bootstrap re-sampling.

T^{sat} (K)	$\rho_{\mathrm{liq}}^{\mathrm{sat}}$ (kg/m^3)	$\rho_{\mathrm{vap}}^{\mathrm{sat}}$ (kg/m^3)	$P_{\mathrm{vap}}^{\mathrm{sat}}$ (MPa)	ΔH_{v} (kJ/mol)	$Z_{\mathrm{vap}}^{\mathrm{sat}}$
490	$423.3_{3.5}$	$87.3_{2.1}$	$25.38_{0.68}$	$14.25_{0.14}$	$0.586_{0.021}$
480	$453.3_{2.0}$	$69.9_{1.5}$	$21.70_{0.60}$	$16.54_{0.12}$	$0.639_{0.022}$
470	$477.4_{1.3}$	$56.51_{0.96}$	$18.44_{0.56}$	$18.448_{0.089}$	$0.686_{0.024}$
460	$497.3_{1.4}$	$46.06_{0.95}$	$15.56_{0.51}$	$20.041_{0.074}$	$0.726_{0.028}$
450	$514.8_{1.3}$	$37.6_{1.3}$	$13.04_{0.44}$	$21.428_{0.10}$	$0.761_{0.037}$
440	$531.5_{1.2}$	$30.7_{1.7}$	$10.84_{0.35}$	$22.71_{0.16}$	$0.792_{0.050}$
430	$547.4_{1.2}$	$25.0_{1.7}$	$8.93_{0.24}$	$23.91_{0.22}$	$0.820_{0.061}$
420	$561.77_{0.87}$	$20.3_{1.5}$	$7.28_{0.13}$	$24.98_{0.23}$	$0.845_{0.063}$
410	$575.17_{0.62}$	$16.34_{0.99}$	$5.875_{0.050}$	$25.97_{0.20}$	$0.867_{0.053}$
400	$588.08_{0.75}$	$13.04_{0.55}$	$4.682_{0.027}$	$26.90_{0.15}$	$0.887_{0.038}$
390	$599.80_{0.63}$	$10.31_{0.28}$	$3.684_{0.047}$	$27.75_{0.11}$	$0.905_{0.027}$
380	$610.32_{0.79}$	$8.06_{0.17}$	$2.858_{0.061}$	$28.507_{0.080}$	$0.922_{0.027}$
370	$621.3_{2.9}$	$6.23_{0.13}$	$2.185_{0.072}$	$29.267_{0.086}$	$0.937_{0.037}$
360	$634.3_{3.1}$	$4.74_{0.11}$	$1.640_{0.083}$	$30.118_{0.078}$	$0.950_{0.053}$

Table SI.XXXI: GCMC-MBAR results for 2-hexyne with the MiPPE force field. Subscripts correspond to the 95% confidence interval computed with bootstrap re-sampling.

T^{sat} (K)	$\rho_{\mathrm{liq}}^{\mathrm{sat}}$ (kg/m^3)	$\rho_{\mathrm{vap}}^{\mathrm{sat}}$ (kg/m^3)	$P_{\mathrm{vap}}^{\mathrm{sat}}$ (MPa)	ΔH_{v} (kJ/mol)	$Z_{\mathrm{vap}}^{\mathrm{sat}}$
500	$438.2_{2.9}$	$85.9_{4.0}$	$24.95_{0.26}$	$14.93_{0.36}$	$0.574_{0.027}$
490	$464.9_{1.8}$	$67.7_{2.5}$	$21.31_{0.16}$	$17.31_{0.29}$	$0.635_{0.024}$
480	$486.7_{1.5}$	$54.7_{1.3}$	$18.11_{0.11}$	$19.18_{0.19}$	$0.682_{0.017}$
470	$505.2_{1.7}$	$44.67_{0.74}$	$15.302_{0.087}$	$20.71_{0.14}$	$0.720_{0.013}$
460	$522.5_{2.3}$	$36.61_{0.52}$	$12.839_{0.074}$	$22.09_{0.14}$	$0.753_{0.012}$
450	$539.3_{2.5}$	$29.96_{0.40}$	$10.686_{0.062}$	$23.39_{0.15}$	$0.783_{0.011}$
440	$555.2_{1.8}$	$24.43_{0.31}$	$8.815_{0.050}$	$24.60_{0.11}$	$0.810_{0.011}$
430	$569.62_{0.68}$	$19.82_{0.28}$	$7.201_{0.040}$	$25.678_{0.066}$	$0.835_{0.013}$
420	$583.3_{1.4}$	$15.98_{0.26}$	$5.821_{0.034}$	$26.69_{0.11}$	$0.857_{0.015}$
410	$597.0_{1.4}$	$12.77_{0.22}$	$4.651_{0.035}$	$27.67_{0.12}$	$0.877_{0.017}$
400	$609.9_{1.1}$	$10.11_{0.16}$	$3.669_{0.039}$	$28.59_{0.11}$	$0.896_{0.017}$
390	$621.7_{1.4}$	$7.92_{0.14}$	$2.857_{0.045}$	$29.42_{0.14}$	$0.914_{0.021}$
380	$633.2_{1.2}$	$6.12_{0.16}$	$2.190_{0.050}$	$30.23_{0.16}$	$0.930_{0.032}$
370	$644.01_{0.40}$	$4.67_{0.18}$	$1.653_{0.059}$	$30.98_{0.19}$	$0.944_{0.049}$

Table SI.XXXII: GCMC-MBAR results for 1-heptyne with the MiPPE force field. Subscripts correspond to the 95% confidence interval computed with bootstrap re-sampling.

T^{sat} (K)	$\rho_{\mathrm{liq}}^{\mathrm{sat}}$ (kg/m^3)	$\rho_{\mathrm{vap}}^{\mathrm{sat}}$ (kg/m^3)	$P_{\mathrm{vap}}^{\mathrm{sat}}$ (MPa)	ΔH_{v} (kJ/mol)	$Z_{\mathrm{vap}}^{\mathrm{sat}}$
520	$427.5_{6.0}$	$82.9_{6.4}$	$22.18_{0.71}$	$16.05_{0.64}$	$0.595_{0.050}$
510	$454.3_{2.5}$	$66.9_{4.8}$	$19.06_{0.55}$	$18.37_{0.49}$	$0.646_{0.050}$
500	$476.5_{1.4}$	$54.5_{3.3}$	$16.29_{0.41}$	$20.34_{0.35}$	$0.691_{0.045}$
490	$495.7_{1.4}$	$44.8_{2.4}$	$13.84_{0.30}$	$22.02_{0.25}$	$0.730_{0.042}$
480	$512.9_{1.6}$	$36.9_{1.8}$	$11.68_{0.20}$	$23.51_{0.18}$	$0.764_{0.040}$
470	$528.7_{2.0}$	$30.3_{1.4}$	$9.79_{0.12}$	$24.85_{0.13}$	$0.794_{0.037}$
460	$543.2_{1.9}$	$24.91_{0.95}$	$8.138_{0.072}$	$26.066_{0.092}$	$0.821_{0.032}$
450	$556.9_{1.5}$	$20.37_{0.57}$	$6.705_{0.058}$	$27.199_{0.070}$	$0.846_{0.025}$
440	$570.2_{1.0}$	$16.57_{0.25}$	$5.472_{0.063}$	$28.279_{0.062}$	$0.868_{0.016}$
430	$583.08_{0.58}$	$13.38_{0.11}$	$4.419_{0.062}$	$29.301_{0.062}$	$0.888_{0.015}$
420	$595.19_{0.32}$	$10.71_{0.23}$	$3.526_{0.055}$	$30.253_{0.097}$	$0.907_{0.024}$
410	$606.63_{0.36}$	$8.50_{0.30}$	$2.779_{0.046}$	$31.14_{0.16}$	$0.923_{0.037}$
400	$617.58_{0.39}$	$6.66_{0.33}$	$2.160_{0.048}$	$31.98_{0.23}$	$0.938_{0.050}$
390	$628.63_{0.36}$	$5.16_{0.31}$	$1.654_{0.061}$	$32.81_{0.31}$	$0.950_{0.067}$

Table SI.XXXIII: GCMC-MBAR results for 1-octyne with the MiPPE force field. Subscripts correspond to the 95% confidence interval computed with bootstrap re-sampling.

T^{sat} (K)	$\rho_{\mathrm{liq}}^{\mathrm{sat}}$ (kg/m^3)	$\rho_{\mathrm{vap}}^{\mathrm{sat}}$ (kg/m^3)	$P_{\mathrm{vap}}^{\mathrm{sat}}$ (MPa)	ΔH_{v} (kJ/mol)	$Z_{\mathrm{vap}}^{\mathrm{sat}}$
550	$419.4_{3.6}$	$89.5_{1.2}$	$20.75_{0.15}$	$16.27_{0.24}$	$0.56_{0.01}$
540	$445.2_{3.0}$	$70.95_{0.88}$	$17.88_{0.15}$	$18.98_{0.20}$	$0.62_{0.01}$
530	$467.6_{2.6}$	$57.19_{0.55}$	$15.35_{0.15}$	$21.30_{0.17}$	$0.67_{0.01}$
520	$487.1_{2.4}$	$46.85_{0.42}$	$13.11_{0.14}$	$23.22_{0.15}$	$0.71_{0.01}$
510	$504.3_{2.0}$	$38.69_{0.48}$	$11.14_{0.12}$	$24.87_{0.13}$	$0.748_{0.012}$
500	$519.8_{1.5}$	$32.01_{0.56}$	$9.395_{0.099}$	$26.33_{0.12}$	$0.778_{0.016}$
490	$534.3_{1.2}$	$26.45_{0.57}$	$7.869_{0.075}$	$27.66_{0.13}$	$0.805_{0.019}$
480	$548.2_{1.2}$	$21.77_{0.52}$	$6.539_{0.053}$	$28.92_{0.15}$	$0.829_{0.021}$
470	$561.6_{1.2}$	$17.83_{0.40}$	$5.385_{0.038}$	$30.10_{0.15}$	$0.852_{0.020}$
460	$574.15_{0.95}$	$14.52_{0.26}$	$4.392_{0.033}$	$31.21_{0.13}$	$0.872_{0.017}$
450	$586.02_{0.57}$	$11.73_{0.12}$	$3.546_{0.033}$	$32.245_{0.084}$	$0.890_{0.012}$
440	$597.51_{0.35}$	$9.404_{0.077}$	$2.830_{0.032}$	$33.229_{0.046}$	$0.907_{0.013}$
430	$608.64_{0.40}$	$7.46_{0.15}$	$2.231_{0.029}$	$34.171_{0.089}$	$0.921_{0.022}$
420	$619.31_{0.42}$	$5.86_{0.20}$	$1.736_{0.027}$	$35.06_{0.16}$	$0.935_{0.036}$
410	$630.00_{0.38}$	$4.55_{0.22}$	$1.330_{0.032}$	$35.94_{0.24}$	$0.946_{0.052}$

Table SI.XXXIV: GCMC-MBAR results for 1-nonyne with the MiPPE force field. Subscripts correspond to the 95% confidence interval computed with bootstrap re-sampling.

T^{sat} (K)	$\rho_{\mathrm{liq}}^{\mathrm{sat}}$ (kg/m^3)	$\rho_{\mathrm{vap}}^{\mathrm{sat}}$ (kg/m^3)	$P_{\mathrm{vap}}^{\mathrm{sat}}$ (MPa)	ΔH_{v} (kJ/mol)	$Z_{\mathrm{vap}}^{\mathrm{sat}}$
570	$427.1_{1.2}$	$80.5_{1.0}$	$17.76_{0.15}$	$18.58_{0.17}$	$0.58_{0.01}$
560	$450.9_{1.3}$	$64.43_{0.86}$	$15.31_{0.13}$	$21.28_{0.20}$	$0.63_{0.01}$
550	$471.7_{1.6}$	$52.31_{0.73}$	$13.15_{0.10}$	$23.58_{0.20}$	$0.683_{0.011}$
540	$489.9_{1.5}$	$43.02_{0.62}$	$11.239_{0.080}$	$25.52_{0.17}$	$0.723_{0.012}$
530	$506.3_{1.1}$	$35.61_{0.52}$	$9.552_{0.059}$	$27.21_{0.13}$	$0.756_{0.012}$
520	$521.47_{0.66}$	$29.51_{0.42}$	$8.067_{0.041}$	$28.739_{0.093}$	$0.785_{0.012}$
510	$535.75_{0.67}$	$24.42_{0.33}$	$6.762_{0.026}$	$30.149_{0.083}$	$0.811_{0.012}$
500	$549.10_{0.85}$	$20.14_{0.26}$	$5.626_{0.015}$	$31.452_{0.094}$	$0.835_{0.011}$
490	$561.65_{0.81}$	$16.54_{0.20}$	$4.64_{0.01}$	$32.666_{0.094}$	$0.856_{0.010}$
480	$573.68_{0.62}$	$13.50_{0.15}$	$3.792_{0.010}$	$33.811_{0.080}$	$0.87_{0.01}$
470	$585.26_{0.49}$	$10.94_{0.11}$	$3.068_{0.014}$	$34.896_{0.067}$	$0.892_{0.010}$
460	$596.35_{0.58}$	$8.794_{0.096}$	$2.455_{0.017}$	$35.924_{0.069}$	$0.907_{0.012}$
450	$607.27_{0.71}$	$7.003_{0.091}$	$1.942_{0.020}$	$36.924_{0.081}$	$0.921_{0.015}$
440	$618.21_{0.61}$	$5.516_{0.091}$	$1.516_{0.023}$	$37.91_{0.10}$	$0.933_{0.021}$
430	$628.74_{0.51}$	$4.292_{0.090}$	$1.166_{0.026}$	$38.85_{0.14}$	$0.944_{0.029}$
420	$638.50_{0.50}$	$3.296_{0.086}$	$0.885_{0.030}$	$39.72_{0.18}$	$0.955_{0.040}$

SI.VII Simulation state points

SI.VII.1 Cyclohexane

Table SI.XXXV: State points simulated for cyclohexane with the MiPPE force field (second iteration, $\theta^{\langle 2 \rangle}$ $\lambda_{\mathrm{CH_2}} = 16$).

T (K)	μ (K)	L (nm)
450	-4367	3.0
500	-4367	3.0
550	-4367	3.0
500	-4149	3.0
460	-4024	3.0
410	-3893	3.0
360	-3792	3.0

Table SI.XXXVI: State points simulated for cyclohexane with the TraPPE force field (zeroth iteration, $\theta^{\langle 0 \rangle}$).

T (K)	μ (K)	L (nm)
450	-4350	3.0
500	-4350	3.0
550	-4350	3.0
500	-4120	3.0
460	-3977	3.0
410	-3790	3.0
350	-3562	3.0

Table SI.XXXVII: State points simulated for cyclohexane with the first iteration ($\theta^{\langle 1 \rangle}$) $\lambda_{\mathrm{CH_2}} = 14$ force field.

T (K)	μ (K)	L (nm)
450	-4389	3.0
500	-4389	3.0
550	-4389	3.0
500	-4164	3.0
460	-4033	3.0
410	-3891	3.0
360	-3780	3.0

Table SI.XXXVIII: State points simulated for cyclohexane with the first iteration ($\theta^{\langle 1 \rangle}$) $\lambda_{\mathrm{CH_2}} = 16$ force field.

T (K)	μ (K)	L (nm)
450	-4367	3.0
500	-4367	3.0
550	-4367	3.0
500	-4149	3.0
460	-4024	3.0
410	-3893	3.0
360	-3792	3.0

Table SI.XXXIX: State points simulated for cyclohexane with the first iteration ($\theta^{\langle 1 \rangle}$) $\lambda_{\mathrm{CH_2}} = 18$ force field.

T (K)	μ (K)	L (nm)
450	-4370	3.0
500	-4370	3.0
550	-4370	3.0
500	-4158	3.0
460	-4037	3.0
410	-3912	3.0
360	-3825	3.0

Table SI.XL: State points simulated for cyclohexane with the first iteration ($\theta^{\langle 1 \rangle}$) $\lambda_{\mathrm{CH_2}} = 20$ force field.

T (K)	μ (K)	L (nm)
450	-4386	3.0
500	-4386	3.0
550	-4386	3.0
500	-4178	3.0
460	-4062	3.0
410	-3946	3.0
360	-3866	3.0

SI.VII.2 Branched alkanes

Table SI.XLI: State points simulated for 2-methylpropane with the TraPPE force field.

T (K)	μ (K)	L (nm)
350	-3120	3.0
380	-3120	3.0
405	-3117	3.0
380	-2980	3.0
350	-2880	3.0
320	-2790	3.0
290	-2705	3.0
260	-2645	3.0
230	-2600	3.0
200	-2570	3.0

Table SI.XLII: State points simulated for 2,2-dimethylpropane with the TraPPE force field.

T (K)	μ (K)	L (nm)
380	-3405	3.0
410	-3405	3.0
440	-3405	3.0
410	-3250	3.0
380	-3140	3.0
350	-3037	3.0
330	-2970	3.0
300	-2900	3.0
270	-2820	3.0

Table SI.XLIII: State points simulated for 2,2-dimethylbutane with the TraPPE force field.

T (K)	μ (K)	L (nm)
420	-3860	3.5
450	-3860	3.5
480	-3860	3.5
450	-3719	3.5
420	-3600	3.5
400	-3524	3.5
380	-3450	3.5
360	-3368	3.5
340	-3288	3.5
310	-3280	3.5

Table SI.XLIV: State points simulated for 2,3-dimethylbutane with the TraPPE force field.

T (K)	μ (K)	L (nm)
440	-4015	3.0
470	-4015	3.0
500	-4011	3.0
470	-3845	3.0
440	-3735	3.0
410	-3635	3.0
380	-3555	3.0
350	-3480	3.0
320	-3415	3.0

Table SI.XLV: State points simulated for 3,3-dimethylhexane with the TraPPE force field.

T (K)	μ (K)	L (nm)
500	-4670	3.5
530	-4670	3.5
560	-4670	3.5
520	-4476	3.5
490	-4370	3.5
460	-4268	3.5
430	-4164	3.5
400	-4039	3.5
370	-3925	3.5

Table SI.XLVI: State points simulated for 3-methyl-3-ethylpentane with the TraPPE force field.

T (K)	μ (K)	L (nm)
500	-4785	4.0
550	-4785	4.0
580	-4785	4.0
550	-4636	4.0
520	-4520	4.0
490	-4400	4.0
460	-4280	4.0
430	-4160	4.0
410	-4080	4.0
390	-3990	4.0

Table SI.XLVII: State points simulated for 2,3,4-trimethylpentane with the TraPPE force field.

T (K)	μ (K)	L (nm)
480	-4740	3.5
520	-4740	3.5
565	-4735	3.5
530	-4549	3.5
500	-4436	3.5
470	-4337	3.5
440	-4241	3.5
410	-4182	3.5
380	-4090	3.5
350	-4020	3.5

Table SI.XLVIII: State points simulated for 2,2,4-trimethylpentane with the TraPPE force field.

T (K)	μ (K)	L (nm)
480	-4600	4.0
530	-4600	4.0
560	-4600	4.0
530	-4450	4.0
500	-4330	4.0
470	-4210	4.0
440	-4090	4.0
410	-3960	4.0
380	-3840	4.0

Table SI.XLIX: State points simulated for 2-methylpropane with the MiPPE-gen force field.

T (K)	μ (K)	L (nm)
350	-3150	3.0
380	-3150	3.0
410	-3145	3.0
380	-3010	3.0
350	-2910	3.0
320	-2830	3.0
290	-2760	3.0
260	-2700	3.0
230	-2670	3.0
200	-2640	3.0

Table SI.L: State points simulated for 2,2-dimethylpropane with the MiPPE-gen force field.

T (K)	μ (K)	L (nm)
368	-3344	3.0
398	-3344	3.0
430	-3400	3.0
398	-3216	3.0
372	-3124	3.0
346	-3032	3.0
326	-2961	3.0
299	-2865	3.0
270	-2759	3.0

Table SI.LI: State points simulated for 2,2-dimethylbutane with the MiPPE-gen force field.

T (K)	μ (K)	L (nm)
415	-3873	3.5
445	-3873	3.5
480	-3895	3.5
450	-3756	3.5
420	-3654	3.5
400	-3588	3.5
380	-3521	3.5
360	-3454	3.5
340	-3384	3.5
310	-3380	3.5

Table SI.LII: State points simulated for 2,3-dimethylbutane with the MiPPE-gen force field.

T (K)	μ (K)	L (nm)
440	-4010	3.0
470	-4010	3.0
500	-4009	3.0
470	-3860	3.0
440	-3760	3.0
410	-3670	3.0
380	-3600	3.0
350	-3530	3.0
320	-3480	3.0

Table SI.LIII: State points simulated for 2,3,4-trimethylpentane with the MiPPE-gen force field.

T (K)	μ (K)	L (nm)
480	-4720	3.5
520	-4720	3.5
565	-4713	3.5
530	-4540	3.5
500	-4360	3.5
470	-4355	3.5
440	-4275	3.5
410	-4205	3.5
380	-4165	3.5
350	-4115	3.5

Table SI.LIV: State points simulated for 2,2,4-trimethylpentane with the MiPPE-gen force field.

T (K)	μ (K)	L (nm)
470	-4570	4.0
520	-4570	4.0
550	-4570	4.0
520	-4420	4.0
490	-4300	4.0
460	-4170	4.0
430	-4050	4.0
400	-3920	4.0
370	-3790	4.0